DIGITAL SIGNAL PROCESSING OF POL-QAM AND SP-QAM IN LONG-HAUL OPTICAL TRANSMISSION SYSTEMS

DONGPENG ZHANG

A THESIS

IN

THE DEPARTMENT

OF

ELECTRICAL AND COMPUTER ENGINEERING

PRESENTED IN PARTIAL FULFILLMENT OF THE REQUIREMENTS

FOR THE DEGREE OF MASTER OF APPLIED SCIENCE

CONCORDIA UNIVERSITY

MONTREAL, QUEBEC, CANADA

February 2014

CONCORDIA UNIVERSITY
SCHOOL OF GRADUATE STUDIES

This is to certify that the thesis prepared

By: Dongpeng Zhang

Entitled: "Digital Signal Processing of POL-QAM and SP-QAM in Long-Haul Optical Transmission Systems"

and submitted in partial fulfillment of the requirements for the degree of

Master of Applied Science

Complies with the regulations of this University and meets the accepted standards with respect to originality and quality.

Signed by the final examining committee:

_____ Chair
Dr. M. Z. Kabir

_____ Examiner, External
Dr. A. Youssef (CIISE) To the Program

_____ Examiner
Dr. Y. R. Shayan

_____ Supervisor
Dr. W. Hamouda

Approved by: _____
Dr. W. E. Lynch, Chair
Department of Electrical and Computer Engineering

2014.2.26 _____
Dr. C. W. Trueman
Interim Dean, Faculty of Engineering
and Computer Science

Abstract

Digital Signal Processing of POL-QAM and SP-QAM in Long-Haul Optical Transmission Systems

Dongpeng Zhang

Coherent detection employing high modulation formats has become one of the most attractive technologies for long-haul transmission systems due to the high power and spectral efficiencies. Appropriate digital signal processing (DSP) is used to equalize and compensate for distortion caused by laser and fiber characteristics and impairments, such as polarization mode dispersion (PMD), polarization rotation, laser phase noise and nonlinear effects. Research on the various DSP algorithms in the coherent optical communication systems is the most promising investigation.

In this research, two new modulation formats; polarization QAM modulation (POL-QAM) and set-partitioning QAM (SP-QAM) are investigated due to their high spectral efficiency and novelty. For PMD and polarization rotation equalization, a new modified constant modulus algorithm (CMA) is proposed for POL-QAM. We investigate the bit error rate (BER) performance of the two modulation formats over fiber channel considering PMD and polarization rotation effects. Furthermore, we investigate the BER performance of the two modulation formats over long-haul fiber optic transmission systems. Carrier phase estimation (CPE) algorithms are also investigated, which are used to mitigate phase noise caused by the transmitter.

Acknowledgments

Foremost, I would like to express my sincere gratitude to my supervisor Dr. Walaa Hamouda for the continuous support of my Master study and research, for his patience, motivation, and immense knowledge. His guidance helped me in all the time of research and writing of this thesis. I could not have imagined having a better advisor and mentor for my Master study.

Besides my supervisor, I would like to thank Dr.Mazen Awad. He spends very much time teaching me the knowledge of optical systems and always showed full confidence in me. Without Dr. Mazen's constructive suggestions and knowledgeable guidance in optical communication and signal processing area, this work would not have been successfully completed.

I thank my friends Anyang Li, Peng Zhang, Qingjiao Song, Hongyan Li, Hang Yu, Zheni Lin, Chao Lu, Haining Zhu, and Yunfeng Gao for the unforgettable time we study together before deadlines. I thank my friends Ming Zhu, Ran Zhu, Meng Zhang, Xinrui Pu, Yiren Li, Yuanjia Jiang, Fei Gao, Feng Guo and Lu Yang for all the fun we have had in the last two years.

I owe more than thanks to my parents for their financial support and continuous encouragements throughout my life. Without their support, it is impossible for me to finish my graduate education seamlessly. I just hope I can live up to their expectations in my future career. Finally, I would like to thank Dr. M. R. xxxx, and Dr. xxxx for serving in my thesis committee.

Contents

List of Figures viii

List of Tables xi

List of Important Symbols xii

List of Acronyms xiv

Chapter 1 Introduction 1

1.1 Optical Communication 1

1.2 Optical Coherent Communication 2

1.3 Motivation 2

1.4 Contributions 3

1.5 Thesis Overview 4

Chapter 2 Fiber Optic Communications 5

2.1 Introduction 5

2.2 Optical Fiber 7

2.2.1 Types of Fiber 7

2.2.2 Fiber Loss 9

2.2.3 Fiber Dispersion 10

2.3 Modulation 12

2.3.1 PDM-QAM 13

2.3.2 POL-QAM 13

2.3.3 SP-QAM 16

2.4 Laser Phase Noise 18
2.5 Nonlinear Effects 20
2.5.1 Self-Induced Phase Modulation 21
2.5.2 Cross-Phase Modulation 21
2.5.3 Four Wave Mixing 22
2.6 Coherent Receiver 24
2.7 Digital Signal Processing Algorithms 25
2.7.1 PMD and Polarization Rotation Equalization 25
2.7.2 Carrier phase recovery 30
2.8 Conclusions 34
Chapter 3 Equalization of POL-QAM and SP-QAM 35
3.1 Introduction 35
3.1.1 Prior Work 36
3.2 System Model 36
3.3 POL-CMA for POL-QAM 38
3.4 Simulation Results 40
3.4.1 Equalization of POL-QAM 6-4 41
3.4.2 Equalization of SP-QAM 45
3.5 Conclusion 50
Chapter 4 Performance in Long-Haul Transmission Systems 52
4.1 Introduction 52
4.2 Erbium Doped Fiber Amplifier 53
4.2.1 EDFA Noise 54
4.3 System Model 55
4.4 Simulation Results 55
4.4.1 Effect of Laser Phase Noise 56

4.4.2 Constellation Change in Long-Haul System..... 61
4.4.3 Equalizer Step Size Optimization 65
4.4.3 System Performance with Different Transmission Length 66
4.4.4 System performance with different fiber lengths..... 68
4.4.5 Amplifier Nonlinear Phase Noise 70
4.5 Conclusions..... 72
Chapter 5 Conclusions and Future Works..... 74
6.1 Conclusions..... 74
6.2 Future Directions 75
Bibliography 76

List of Figures

2.1 Optical fiber communication chain

2.2 Digital signal processing architecture

2.3 Optical fiber structure

2.4 Generation of PDM-4QAM signals

2.5 POL-QAM 6-4 constellation

2.6 Modulator architecture of POL-QAM 6-4

2.7 An example of mapping 110110011 to two symbols

2.8 The transmitter structure of SP-128-QAM and PDM-16-QAM

2.9 An example of mapping 1101011 in 128-SP-QAM format

2.10 An example of constellation change of POL-QAM 6-4 distorted by laser phase noise

2.11 Equalization of dual-channel modulation

2.12 Schematic of CMA equalizer

2.13 Phase unwrapping

2.14 Block diagram of Viterbi&Viterbi phase recovery algorithm

2.15 Block diagram of DD carrier phase recovery algorithm

3.1 Optical system model

3.2 Block diagram of POL-CMA architecture

3.3 POL-QAM 6-4 constellation change during equalizing

3.4 POL-QAM BER with step size of POL-CMA and LMS

3.5 Mean Square Error of POL-CMA for POL-QAM

3.6 BER performance of POL-QAM 6-4 with POL-CMA and LMS

3.7 128-SP-QAM constellation change during equalizing

3.8 128-SP-QAM BER for MMA and LMS

3.9 Mean Square Error (MSE) of MMA for 128-SP-QAM

3.10 BER Performance of 128-SP-QAM as a function of fiber length

3.11 BER Performance of 128-SP-QAM and PDM-16-QAM with variable fiber length equalized by MMA

4.1 Schematic diagram of EDFA

4.2 Architecture of long-haul system model

4.3 POL-QAM 6-4 constellation changes in a fiber system considering laser phase noise effect and compensation algorithms

4.4 128-SP-QAM constellation changes in a fiber system

4.5 BER performances of POL-QAM 6-4 considering laser phase noise using carrier phase estimation algorithms with different fiber length

4.6 BER performances of 128-SP-QAM and PDM-16QAM considering laser phase noise using DD with different fiber length

4.7 POL-QAM 6-4 x-polarization constellation changes in long-haul system

4.8 128-SP-QAM x-polarization constellation changes in long-haul system

4.9 The BER performances with the step size of POL-CMA and LMS for POL-QAM

4.10 The BER performances with the step size of MMA and LMS for 128-SP-QAM

4.11 POL-QAM 6-4 and PDM-4QAM BER performance with different fiber length in long-haul systems

4.12 128-SP-QAM and PDM-16QAM BER performance with different fiber length in long-haul systems

4.13 POL-QAM 6-4 and PDM-4QAM BER performance with different fiber span length in long-haul systems

4.14 128-SP-QAM and PDM-16QAM BER performance with different fiber span length in long-haul systems
4.15 POL-QAM 6-4 and PDM-4QAM BER performance with different fiber length in long-haul systems, consider nonlinear phase noise as amplifier noise
4.16 128-SP-QAM and PDM-16QAM BER performance with different fiber length in long-haul systems, consider nonlinear phase noise as amplifier noise

List of Tables

2.1 Comparison of Modulation Formats.

2.2 The 9-bits symbol mapping for POL-QAM 6-4

2.3 Comparison of SPM, CPM and FWM

List of Important Symbols

IQ	in-phase and quadrature
α	attenuation factor
P	power of signal
P_0	launched power at the transmitter of the fiber,
L	fiber distance.
J	Jones Matrix
θ	angular frequency.
$\tilde{n}$	e□ective refractive index of the fiber
n	linear refractive index
I	optical intensity
n_2	nonlinear-index coefficient.
ϕ	phase of signal
λ	laser wavelength
k_0	laser frequency
ϕ_{NL}	Non-linear phase shift
ω	frequency of optical field
Δ_k	Gaussian distributed random variable value

$\Delta\nu$	sum of the carrier laser and receiver local oscillator 3-dB linewidths
T_s	symbol period
ϕ_k^{NL}	nonlinear phase distortions and noise
M	Number of symbols in modulation constellation
B	bandwidth of coherent receiver
N	equalizer tap length
μ	equalizer step size
R	information bit rate
W	block length of carrier phase recovery algorithm
$\Delta\nu$	laser linewidth
F_n	amplifier noise figure
h	Planck constant
G	amplifier gain
n_{SP}	spontaneous emission factor
N_1	atomic population of the ground
N_2	atomic population of the excited states
N_{amp}	number of amplifiers
A	amplitude of the transmitted signal
e	electron charge
R_P	responsivity of photodiodes
P_{LO}	power of local oscillator
k	Boltzmann constant
T	temperature

List of Acronyms

4D	four-dimensional
ASE	amplified spontaneous emission
ASK	amplitude shift keying
CMA	Constant Modulus Algorithm
CPE	carrier phase estimation
DD	Decision-Directed
DP	Dual-Polarization
DSP	digital signal processing
EDFA	Erbium Doped Fiber Amplifier
FSK	frequency shift keying
I and Q	in-phase and quadrature field components
IM/DD	intensity modulation with direct detection
LMS	Least Mean Square
LO	local oscillator
MAN	metropolitan area network
ML	maximum-likelihood
MMA	Multimodulus Algorithm
NRZ	Non Return to Zero
PBC	polarization beam combiner
PBS	polarizing beam splitter
PDM-16QAM	polarization division multiplexed 16-QAM
PDM-QPSK	polarization division multiplexed quaternary phase shift keying
PDM-4QAM	polarization division multiplexed 4 quadrature amplitude modulation
PLL	phase-locked loop

PMD	Polarization mode dispersion
POL-CMA	Polarization Constant Modulus Algorithm
POL-QAM	Polarization QAM modulation
PSK	phase shift keying
QAM	quadrature amplitude modulation
RS	Reed-Solomon
RZ	Return to Zero
SNR	signal to noise ratio
SOP	state-of-polarization
SPM	Self-induced phase modulation
SP-QAM	Set-partitioning QAM
V&V	Viterbi&Viterbi
XPM	Cross-phase modulation
ZF	zero-forcing

Chapter 1

Introduction

1.1 Optical Communication

Optical communication systems go back to the 1960s due to the discovery of lasers and fibers [1][2]. At that time, optical fiber was not employed to transmit optical signals in long distances due to its unacceptable high attenuation of around 1000dB/km [3][4]. However, in the early 1970s, Corning Glass Works [5] invented new types of fiber which reduced the fiber attenuation to 20dB/km at wavelength $\lambda = 1.55\mu m$, which was a great improvement of optical communication. The first GaAs semiconductor laser was invented around that time [6].

A simple digital modulation scheme for optical communication systems named intensity modulation with direct detection (IM/DD), which utilizes the intensity of optical carrier to transmit electrical bit stream and reverts to electrical domain at the receiver using a photodiode, plays an important role in lightwave systems since 1970s. The advantage of IM/DD is that the receiver sensitivity is independent of the carrier phase of the optical signal [7]. However, the receiver part of IM/DD provides good power efficiency only at

low spectral efficiency due to the fact that IM/DD limits the degrees of freedom for encoding of information [8]. In the modern time, higher date rate and higher spectral efficiency become significant in optical communication systems. A number of alternative transmission schemes [9][10][11] were proposed in order to improve the problems of traditional IM/DD. Coherent transmission systems were explored during 1980s due to the gradually increased importance of phase coherence of optical carrier [12]-[16].

1.2 Optical Coherent Communication

With the introduction of the Erbium Doped Fiber Amplifier (EDFA) at early 1990s, longer non-regenerated distance can be achieved by amplifying the optical signal and higher sensitivity can be achieved by pre-amplifying the received signal.

Moreover, direct detection which is integrated with EDFA pre-amplification shows similar performance compared with coherent detection. To this end, further research in coherent optical communications had practically been interrupted for some time. Coherent technologies have restarted to attract a large interest over the recent years [17][18][19]. The motivation of that is to fulfill the increased bandwidth requirement with high level modulation formats based on coherent communication.

The benefit of coherent transmission systems is obvious. The coherent receiver sensitivity increased by 20dB compared to IM/DD [20], which allows longer transmission distance. The more important improvement is the ability to employ a variety of spectrally efficient modulation formats, such as quadrature amplitude modulation (QAM) [7]. These modulation formats should have enough high power efficiency and relatively low implementation complexity on both transmitter and receiver sides.

1.3 Motivation

Recent studies on optical communications mainly focus on high level modulation formats

in order to improve the spectral efficiency and increase the transmission speed. To analyze new high level modulation format in fiber transmission, the compensation of channel distortion is an important task.

Due to the fact that optical coherent communication has the ability to detect both the amplitude and the phase of the received signal, a variety of modulation formats which utilize amplitude, phase or frequency for modulation can be implemented. The corresponding modulation formats are amplitude shift keying (ASK), phase shift keying (PSK) and frequency shift keying (FSK), respectively [9][21][22]. In 2009, a new type of modulation format, named Polarization QAM modulation (POL-QAM) was introduced by Henning Bülow [23]. In [23], an introduction of the constellation diagram was given followed by sensitivity analysis of this new modulation format. With a simplified detection algorithm based on a maximum-likelihood (ML) detection model, simulation results showed the coded POL-QAM has a 1.7dB higher sensitivity and 14% higher spectral efficiency compared to the tradition polarization division multiplexed (PDM) 4QAM [23], This modulation format is based on two QPSK signals transmitted over two channels separately. Another newly proposed modulation format, named set-partitioning QAM (SP-QAM), has a higher power efficiency of 2.45 dB compared with PDM-16QAM at a fixed bit rate [24].

This thesis explores POL-QAM and SP-QAM, where we study the performance of 112Gb/s POL-QAM 6-4 and SP-128-QAM using efficient equalization algorithms.

1.4 Contributions

This thesis investigates the performance of POL-QAM 6-4 and SP-128-QAM using efficient equalization algorithms. Furthermore, in long-haul transmission channel, carrier phase estimation is investigated through simulations. The primary contributions are summarized as follows:

- A blind equalization algorithm designed for a high level modulation format is proposed and analyzed.
- Digital signal processing algorithms for high level modulation formats are presented and analyzed.
- We compare the performance of new high level modulation formats with traditional modulation formats.
- We investigate the performance of digital signal processing algorithms for high level modulation formats in long-haul optical transmission.

1.5 Thesis Overview

The thesis is organized as follows. In Chapter 2, the description of the general optical transmission system model is given. Furthermore, we review various digital signal processing algorithms, such as equalization algorithms and carrier phase recovery algorithms.

In Chapter 3, the BER performances of POL-QAM 6-4 and 128 SP-QAM considering channel distortion are presented. A new equalization algorithm is investigated, which is used to mitigate PMD and polarization effects for POL-QAM 6-4. The BER performance of 128-SP-QAM is also investigated using equalization.

In Chapter 4, the system performance under EDFA and laser phase noise is studied. This thesis gives a specific simulation of POL-QAM and SP-QAM systems under EDFA elements which cause amplified spontaneous emission (ASE) noise and amplifier nonlinear phase noise. Laser phase noise and the corresponding Viterbi&Viterbi (V&V) carrier phase estimation (CPE) algorithm are also considered in the simulations (Decision-Directed CPE is used for SP-128-QAM). The performance comparison of V&V and DD for POL-QAM is also studied under amplifier non-linear phase noise.

Finally, Chapter 5 gives conclusions and future work.

Chapter 2

Fiber Optic Communications

2.1 Introduction

In coherent optical communication systems, the fiber impairments are divided into linear and nonlinear effects. This chapter gives a brief description of the fiber optic transmission channel and also introduces the solutions for the main effects.

Figure 2.1 shows a block diagram of an optical communication chain. The key elements of the optical communication system are transmitter block, optical channel and receiver block. The transmitter consists of optical source, modulation and drive circuit.

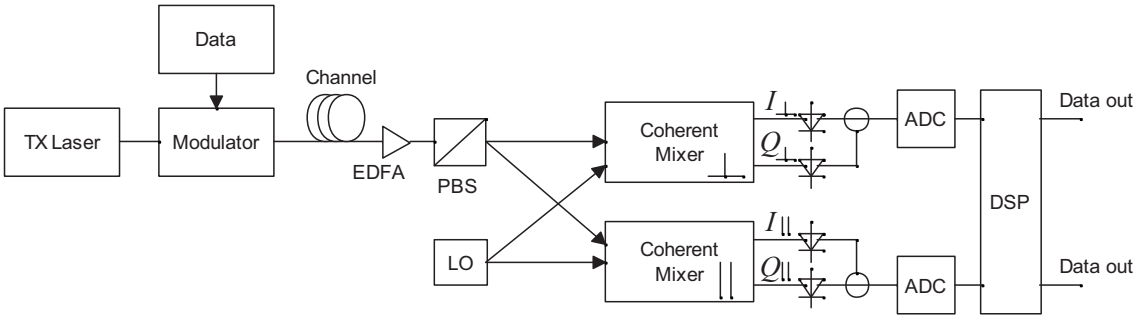

Figure 2.1 Optical fiber communication chain

In the transmitter block, data is generated and sent to drive circuit to represent the signal in Return-to-Zero (RZ) or Non-Return-to-Zero (NRZ) format. The output of the drive circuit and light source are sent to modulator to modulate the optical signal. Connectors are used to provide the interface between transmitter block and the fiber link (so as fiber and receiver block). The optical channel comprises of optical fiber as transmission medium and optical amplifier to amplify the transmitted signal. The optical amplifier is used to enhance the optical signal power without converting to electrical signal. At the receiver side, a coherent receiver is used to sense the light signals and convert them back to electrical signals. Also digital signal processing is employed to extract the signal from noise-induced signal as shown in Figure 2.2.

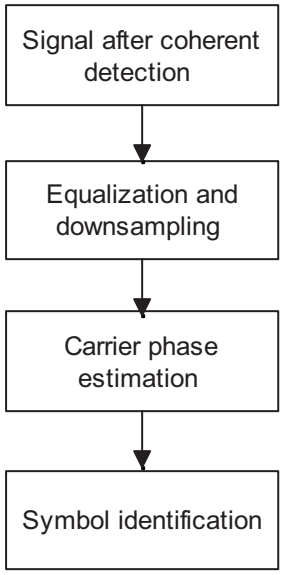

Figure 2.2 Digital signal processing architecture

2.2 Optical Fiber

2.2.1 Types of Fiber

An optical fiber is normally made up with a core, cladding and buffer coating where the core carries light pulses, the cladding reflects light pulses back into the core and the coating is made to cover core and cladding for safety issues. Optical fiber offer many advantages over the copper wires as it can transmit the data over longer distance with low probability of error, higher bandwidth and high resistance to electromagnetic noise. The basic structure of an optical fiber is shown in Figure 2.3.

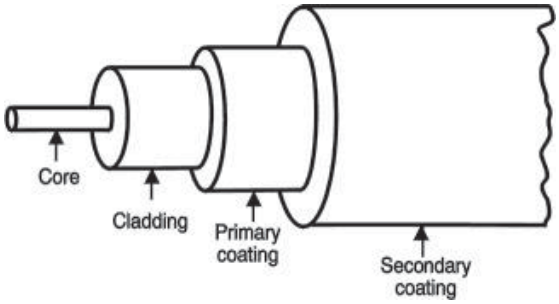

Figure 2.3 Optical fiber structure [25]

As shown in Figure 2.3, the diameter of the core is smaller than the cladding and coating. The basic parameter of optical fiber is its refractive index, defined as the ratio of light speed to the phase velocity of the wave in the medium which varies with respect to different mediums.

Step index fiber and graded index fiber are two types of fibers depending on the material variations of the core. In step index fiber, uniform refractive index of core is maintained throughout the fiber and abrupt change is seen at cladding boundary, which results in light rays arriving separately at the receiver. This is the basic mechanism of optical fibers. On the other hand, in graded index fiber, the refractive index of the core varies with the radial distance from fiber axis which is not constant but decreases gradually from its maximum at the core center to its minimum at the core-cladding interface. Most graded index fibers have a nearly quadratic decrease in the core index. These fibers are further divided into single mode (also called monomode) and multimode fibers with respect to step and graded index fiber. Single mode fiber carries only one mode of light propagation while a multi-mode fiber carries a number of modes. However with multimode step index fiber, signals arrive at different times resulting in pulse spreading causing “intermodal dispersion”. To overcome the dispersion in step index fiber, multimode graded index fiber is often used.

2.2.2 Fiber Loss

In a long-haul transmission system, fiber loss is an inevitable phenomenon which weakens the power of the received signal. Fiber attenuation, material absorption and Rayleigh scattering are normally studied as the main effects of fiber loss.

(1) **Attenuation**

Similar to electrical communication, the power of symbols decreases as the transmission distance increases in fiber communication as given by (2.2.2). The attenuation factor α is used to describe the power loss in fiber.

$$P = P_0 e^{-\alpha L} \tag{2.2.2}$$

where P is the power of the signal, P_0 is the launched power at the transmitter of the fiber, and L is the distance traveled by the signal. The attenuation factor α is usually expressed in [dB/km] and varies with the optical wavelength. α reaches a minimum at 1550nm wavelength, which is around 0.17 dB/km. It is known that fiber attenuation is often compensated by optical amplifiers such as EDFA.

(2) **Material Absorption**

Material absorption is a significant factor of signal loss in fiber communications. Attenuation results when light is absorbed at particular wavelengths, which is converted and dissipated in the form of heat energy. Material absorption is divided into intrinsic and extrinsic material properties. Intrinsic absorption occurs when there are no imperfections and impurities in an optical fiber and this sets the minimum level of absorption. It corresponds to absorption by fused silica. On the other hand, extrinsic absorption is caused by impurities (such as Fe, Cu, Co, etc.) in the optical fiber during manufacturing. Extrinsic absorption occurs by electronic transition of ions from one energy level to

another. Both intrinsic and extrinsic absorption exists in any region of wavelengths.

2.2.3 Fiber Dispersion

The shape of optical pulses is widened with time after a long haul transmission in the fiber. This pulse broadening effect is called fiber dispersion. It is know that the system capacity is proportional to the number of pulses sent per unit time. In what follows, we discuss chromatic dispersion and polarization mode dispersion.

(1) **Chromatic dispersion**

Chromatic dispersion is a phenomenon in fiber optic communications. The time difference of different input wavelengths in a light beam causes chromatic dispersion. Material dispersion and waveguide dispersion are generally two sources of chromatic dispersion. Material dispersion comes from a frequency-dependent response of a material to waves whereas, waveguide dispersion occurs when the speed of a wave in the fiber depends on its frequency for geometric shape reasons. Specifically, waveguide dispersion depends on fiber constitution characteristics (core radius etc.). The general expression of chromatic dispersion is normally expressed in-terms of the temporal pulse spreading per unit bandwidth per distance travelled (ps/nm/km), however, this parameter is ordinarily calculated by the time delay between the wavelength differences after fiber propagation.

Chromatic dispersion becomes a main consideration and must be considered when developing optical fibers. The compensation methods were explored as two ways: (1), Pre-compensating the optical signal before transmission; (2), Use dispersion compensating fiber. This thesis does not consider chromatic dispersion as an effect of channel because the research works of chromatic dispersion and its corresponding compensating algorithms have already been proposed in the literature.

(2) **Polarization Mode Dispersion**

PMD arises from the birefringence effect of optical fiber, which makes the fiber

refractive index dependent on polarization. For ideal optical fiber (no impurities), the basic mode signal has two orthogonal polarizations which propagate at the same speed. However, in a real fiber, the two polarizations do not always propagate at the same speed due to random imperfections that break the circular symmetry of the core. Elliptical cores are normally caused by imperfections in manufacturing or mechanical stresses.

In single mode fiber, polarization mode dispersion (PMD) plays a significant role which may distort the pulse width at the receiver, which also limits the transmission bandwidth. In the literature, many researchers have studied the theoretical and experimental foundations of PMD in the fiber [26]-[30].

The PMD and fiber polarization rotation effects can be measured as a function of wavelength and time by using Jones matrix [31]. The 2x2 Jones matrix is a simple shorthand structure used to represent the polarization state of light when the optical transmission channel is a dual-channel system. Jones matrix is a unitary operator which considers the polarization evolution in the optical component (fiber) due to coupling between the polarization modes [32]. The 2x2 Jones matrix is described as follows [33]:

$$\mathrm{J} = \begin{pmatrix} \cos(\theta) & \sin(\theta) \\ -\sin(\theta) & \cos(\theta) \end{pmatrix} \tag{2.2.3a}$$

where θ is the angular frequency.

Equation (2.2.3b) presents the Jones matrix as multiplicative to the signal.

$$\mathrm{E}_{out}(t) = \mathrm{J} \bullet E_{in}(t) \tag{2.2.3b}$$

where E_{out} is the output signal of the channel, E_{in} is the input signal to the channel.

2.3 Modulation

An important goal of a long-haul optical communication system is to transmit at high data rate over the longest distance without signal regeneration. Spectral efficiency maximization has become significant due to the limitation of optical amplifier bandwidth and fiber impairments [34]. In high level modulation formats with all four dimensions of the incoming optical field (amplitude, frequency, phase and polarization), coherent detection combined with DSP, can lead to increase in capacity and high spectral efficiency [35]. In exchange for such advantages, coherent receivers are sensitive to the phase (nonlinear effect of the fiber, amplifier phase noise, laser phase noise) and state-of-polarization (SOP) of the incoming signal. In order to deal with this problem, the structure of coherent systems becomes much more complicated than that of IM/DD systems. In addition, low optical power (to decrease the nonlinear impairment effect of the fiber) requires high receiver sensitivity that is a parameter crucial to determining the capacity of an optical communications network. Table 2.1 shows the comparison of different modulation formats for bit rate 112Gb/s [23][24].

Table 2.1 Comparison of modulation formats.

Modulation Format	Bit/symbol	Baud value (GHz)
PDM-4QAM	4	28
POL-QAM 6-4	4.5	25
PDM-16QAM	8	14
128 SP-QAM	8	14

In this thesis we use single mode fiber since our work is focused on four-dimensional (4D) modulation format (POL-QAM and SP-QAM), which transmits two independent constellations in each of the two orthogonal polarization states of the fiber. Also single

mode fibers are chosen to transmit the signal because we only consider metropolitan area network (MAN).

In this thesis, Polarization QAM Modulation (POL-QAM) and set-partitioning QAM (SP-QAM) are introduced due to their high spectral efficiency [23]. The detailed description of POL-QAM and SP-QAM are presented below along with the PDM-QAM as it is used for comparison.

2.3.1 PDM-QAM

Through polarization multiplexing, the fiber can use two orthogonal polarization states to transmit two independent QAM signals. The modulation format using this method is named PDM-QAM. Figure 2.4 shows the generation of PDM-4QAM. As shown in Figure 2.4, the light signal from the laser is modulated into two 4QAM optical signals using two Mach-Zehnder modulators after the polarizing beam splitter (PBS). The two orthogonally polarized signals are then integrated into the fiber by the polarization beam combiner (PBC) [36].

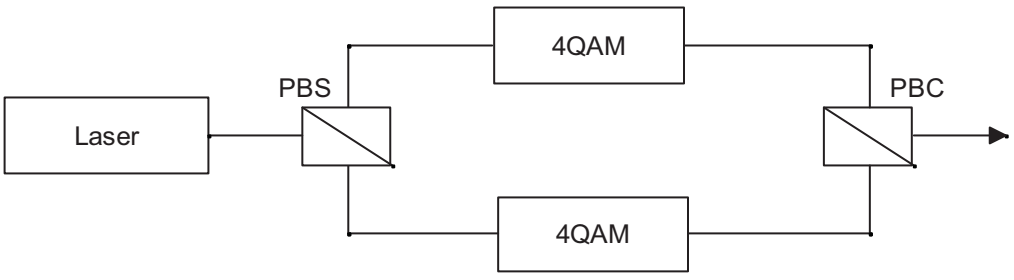

Figure 2.4 Generation of PDM-4QAM signals

2.3.2 POL-QAM

This new type of modulation format which is called polarization QAM (POL-QAM) was

introduced in 2009 [23]. It is based on polarization division multiplexed quaternary phase shift keying modulation (PDM-QPSK). For instance, POL-QAM 6-4 constellation occupies 6 state-of–polarizations (SOPs), which has two more SOPs than PDM-QPSK. It is worth noting that for POL-QAM 6-4, the first number "6" indicates 6 SOPs in the constellation and the last number "4" indicates 4 constellation points in each IQ diagram [23]. Figure 2.5 shows the constellation of POL-QAM 6-4.

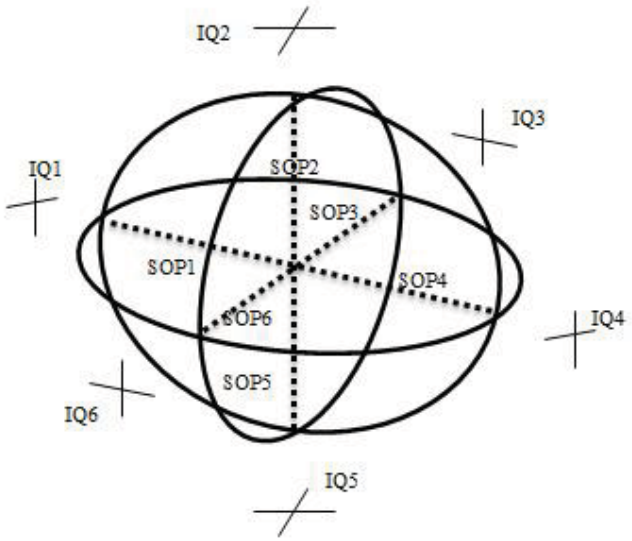

Figure 2.5 POL-QAM 6-4 constellation

The two additional SOPs extend the symbol alphabet without losing sensitivity. Figure 2.6 shows the modulator architecture of POL-QAM 6-4 [23]. In Figure 2.6, the modulator D_0 has three output states.

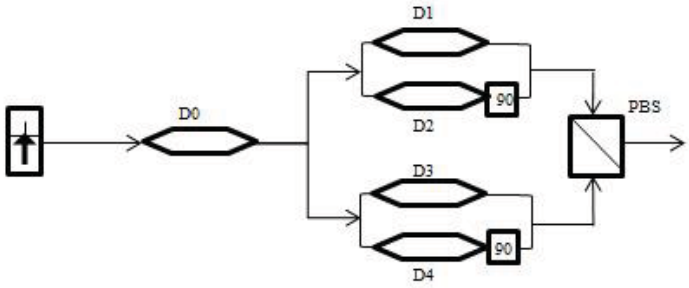

Figure 2.6 Modulator architecture of POL-QAM 6-4

Table 2.2 shows the symbol mapping rules for POL-QAM 6-4.

Table 2.2 The 9-bits symbol mapping for POL-QAM 6-4

b0	b1	b2	b3	b4	b5	b6	b7	b8
0	IQ_{x1}(b1,b2)		IQ_{y1}(b3,b4)		IQ_{x2}(b5,b6)		IQ_{y2}(b7,b8)	
1	0	0	$\sqrt{2}$ • IQ_{x1}(b3,b4), y1=0		IQ_{x2}(b5,b6)		IQ_{y2}(b7,b8)	
1	0	1	$\sqrt{2}$ • IQ_{y1}(b3,b4), x1=0		IQ_{x2}(b5,b6)		IQ_{y2}(b7,b8)	
1	1	0	$\sqrt{2}$ • IQ_{x2}(b3,b4), y2=0		IQ_{x1}(b5,b6)		IQ_{y1}(b7,b8)	
1	0	1	$\sqrt{2}$ • IQ_{y2}(b3,b4), x2=0		IQ_{x1}(b5,b6)		IQ_{y1}(b7,b8)	

In this table, the entry IQ_{x1}(b1,b2) means mapping bit b1 and b2 following 4QAM mode in the first symbol of the x-polarization. Similarly, IQ_{y2}(b7,b8) means mapping bit b7 and b8 following 4QAM mode in the second symbol of the y-polarization.

Figure 2.7(a)-(d) show the constellation diagram of mapping 110110011 in POL-QAM 6-4 format. Using the format in Table 2.2 with b0=1, b1=1,b2=0; then b3 and b4 bits (1,1) are mapped in the second symbol of the x-polarization with $\sqrt{2}$ increase in signal level; the b5 and b6 bits (0,0) are mapped in the first symbol of the x-polarization; the b7 and b8 bits (1,1) are mapped in the first symbol of y-polarization; and the second symbol of

the y-polarization is zero.

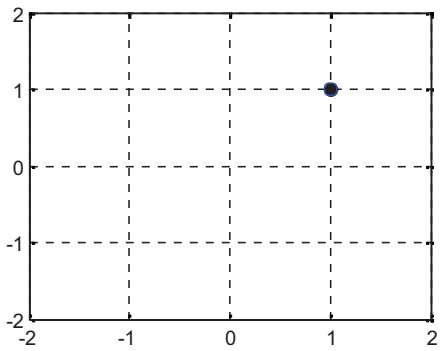

(a) 1st symbol in x-polarization

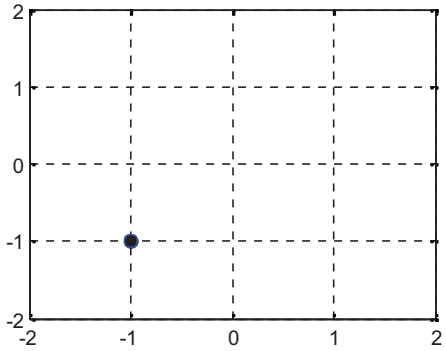

(b) 1st symbol in y-polarization

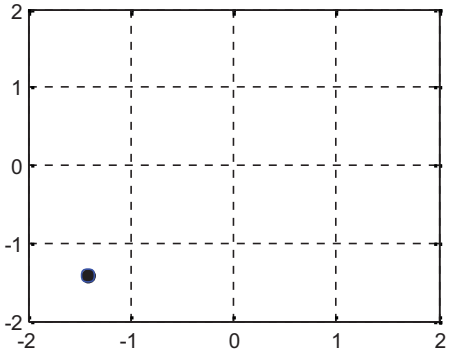

(c) 2nd symbol in x-polarization

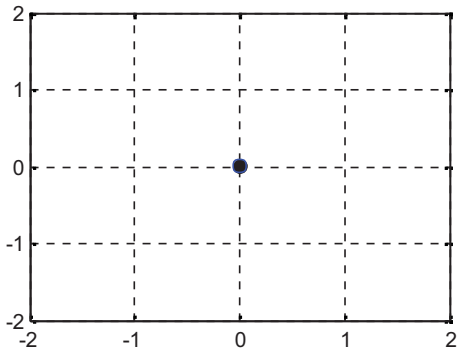

(d) 2nd symbol in y-polarization

Figure 2.7 (a)-(d) An example of mapping 110110011 to two symbols

2.3.3 SP-QAM

In 2011, Coelho and Hanik [37] introduced two modulation formats to coherent optical communication by using Ungerboeck set-partitioning scheme to PDM-16QAM [24]: set-partitioning 32 PM-16QAM (32-SP-QAM) and set-partitioning 128 PDM-16QAM (128-SP-QAM). Compared with PDM-16QAM, 128-SP-QAM has comparable spectral efficiency (7 bits per symbol). Recently, M. Sjodin *et al*. [38] presented comparison of 128-SP-QAM and PDM-16QAM in long-haul transmission systems, by studying

numerical simulations of the nonlinear Schrodinger equation. Both non-differential coding and differential coding with 128-SP-QAM are presented and a great advantage of BER performance is also presented.

Calculating the power efficiency [39], 128-SP-QAM offers power efficiency of −1.55 dB compared to PDM-QPSK (also called PDM-4QAM) and +2.45 dB compared to PDM-16QAM at an exact bit rate [40].

Non-differential coding and differential coding are normally used to encode 128-SP-QAM. This thesis focuses on non-differential coding with 128-SP-QAM as follows.

Non-differentially encoded 128-SP-QAM is generated by taking the even parity subset or the odd parity subset from PDM-16QAM. Then a parity bit is created by performing an XOR operation on the information bits for each of the 7 information bits. Then the eight bits (the parity bit is right after the information bits) is Gray encoded to dual-polarization 16QAM [38]. The transmitter of 128-SP-QAM and PDM-16QAM are presented in [38]: Figure 2.8 shows the structure of 128-SP-QAM.

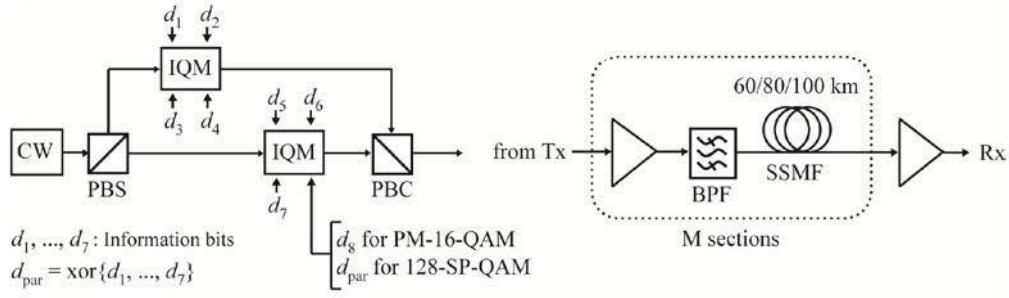

Figure 2.8 The transmitter structure of 128-SP-QAM [38]

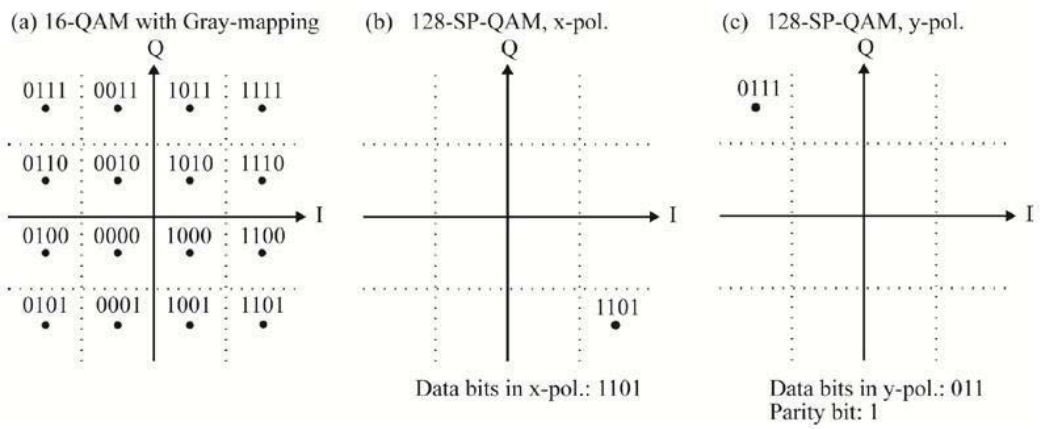

(a) (b) (c)

Figure 2.9 An example of mapping 1101011 in 128-SP-QAM format (a) 16-QAM with Gray-mapping. (b) and (c) show an example of non-differential coded of information bits 1101011 [38]

Figure 2.9 shows constellation diagram of mapping 1101011 in 128-SP-QAM format.

In order to decode the 128-SP-QAM symbol with non-differential coding, an algorithm introduced by J. H. Conway and N. J. A. Sloane [41] is used. The algorithm (algorithm 2 [41]) to decode one symbol can be described in 3 steps:

1. Gray-decode the 16-QAM symbols in two polarizations to obtain eight bits.

2. Move the most uncertain bit of the 4D signal over the closest decision threshold. Decode the 4-D signal to obtain the second eight bits.

3. Check the parity bit of the two bit sequences (one is even and the other is odd). Keep the one with even parity. Discard the parity bit to obtain 7 information bits.

After selecting the modulation format of the transmitter, the signal is transmitted through the fiber and then received by the coherent receiver.

2.4 Laser Phase Noise

Laser phase noise is a phenomenon which results from randomly occurring spontaneous emission in the transmitter laser and the local oscillator laser. It cannot be avoided but can

be modeled by Wiener process since the mean squared phase deviation increases linearly with time [42]. It can be modeled as follows:

$$\theta_{\mathrm{k}} = \theta_{k-1} + \Delta_k \tag{2.6}$$

where θ_{k} is the phase offset of the k-th symbol, Δ_k is a Gaussian distributed random variable with zero mean and variance $\sigma_{\Delta}^2 = 2\pi\Delta\nu\mathrm{T}_{\mathrm{s}}$. $\Delta\nu$ is the sum of the carrier laser and receiver local oscillator 3-dB linewidths. T_{s} is the symbol period. It is known that laser phase noise can be compensated by carrier phase recovery algorithms. The phase noise effect for 112GHz POL-QAM signal is shown in Figure 2.10.

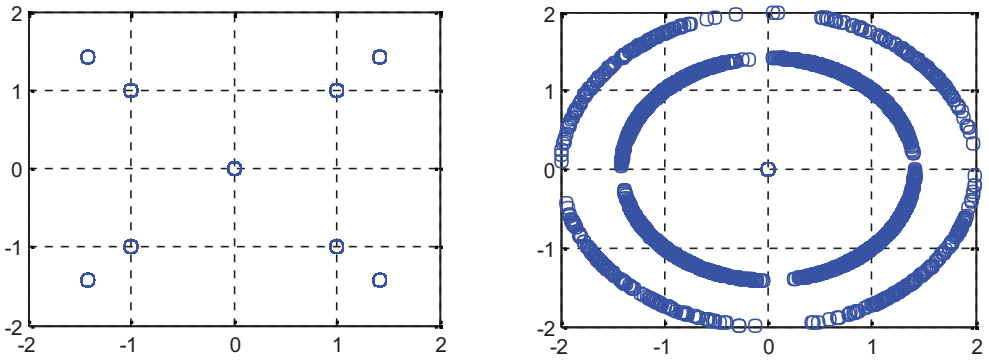

(a) (b)

Figure 2.10 An example of constellation change of POL-QAM 6-4 distorted by laser phase noise (a) Constellation of POL-QAM 6-4 in x-polarization. (b) Laser phase noise effect for 112Gb/s POL-QAM signal

Laser phase noise is a crucial impairment in the coherent optical communication system, since it affects the carrier synchronization between the transmitter laser and the local oscillator laser. Carrier phase is not significant in IM/DD system because the IM/DD receiver only detects the power of the optical signal without detecting carrier phase. In coherent optical systems, the information bits are modeled with variation of carrier phase,

by this reason, the phase shift over a symbol period has critical influence on signal demodulation.

Figure 2.10 shows that the 112Gb/s POL-QAM 6-4 constellation is interfered significantly by laser phase noise. In traditional optical coherent systems, the laser phase noise is normally compensated by using the optical Phase-Lock Loops (PLL) in the receiver to estimate the phase variation with time. Recently the carrier phase noise can be compensated by using DSP algorithms, such as the feed-forward and feed-back carrier phase estimation. For example, Viterbi&Viterbi (V&V) algorithm [43] is a feed-forward algorithm which will be discussed later.

2.5 Nonlinear Effects

In an optical system, optical fiber nonlinearity is caused by high intensity of light in the core. Raman scattering phenomenon and change in the refractive index of the medium related with the intensity of optical signal are the two main sources of nonlinear effects in optical fiber [44].

This section gives a description of fiber nonlinear effects: self-induced phase modulation (SPM) and cross-phase modulation (XPM). The effective refractive index of the fiber mode always described as follows [45]:

$$\tilde{n}(\omega, I) = n(\omega) + n_2 I \tag{2.5}$$

In (2.5), $n(\omega)$ explains the linear part, I is the optical intensity, and n_2 is the nonlinear-index coefficient.

2.5.1 Self-Induced Phase Modulation

Nonlinear effect normally depends on the intensity of optical signal and refractive index. The high light intensity of input pulse in the fiber core results in high refractive index. Also the change of the signal intensity with respect to time results in variations in refractive index. These variations in refractive index cause time dependent phase changes [44]. Here self-induced phase modulation (SPM), refers to the self-induced phase shift experienced by an optical field during its propagation in optical fibers. The magnitude can be obtained by noting that the phase of an optical field changes as [45]

$$\phi = (n + n_2 I)k_0 L \tag{2.5.1}$$

In (2.5.1), $k_0 = \frac{2\pi}{\lambda}$, λ is the wavelength, L is the distance of communication. Hence SPM nonlinear phase shift is $\phi_{\mathrm{NL}} = n_2 I k_0 L$.

In SPM, pulse broadening is seen in the time domain and spectral characteristics are fixed. The Chirp produced by SPM is used to decrease the effects of dispersion which caused by pulse broadening. It is known that SPM is a main limitation in single channel optical systems.

2.5.2 Cross-Phase Modulation

Cross-phase modulation (XPM or CPM), which is a nonlinear optical effect where one wavelength of light can affect the phase of another wavelength of light through the optical Kerr effect. XPM is similar to SPM besides it appears when there are more than one optical signal transmitted in the fiber. XPM is probable caused by asymmetric spectral broadening and pulse shape distortion [44]. Consider two optical fields

propagating simultaneously; nonlinear refractive index seen by one wave depends on the intensity of the other wave as described by [45]:

$$\Delta n_{NL} = n_2(I_1 + bI_2)$$

(2.5.2a)

where I_1 and I_2 are intensities of the optical signals. The nonlinear phase shift is given by [45]:

$$\phi_{NL} = (2\pi L / \lambda)n_2\left[I_1 + bI_2\right] \quad (2.5.2b)$$

The fiber nonlinear effects are difficult to compensate for in traditional high speed intensity modulation with direct detection (IM/DD) transmission systems. In digital coherent systems, the nonlinear effects can be mitigated by using the backward propagation methods based on solving the nonlinear Schrödinger equation and the Manakov equation [46][47].

2.5.3 Four Wave Mixing

In optical fiber, when three optical fields transmitted through a fiber, a new optical field which depends on the three optical fields will be produced. This effect is called four wave mixing (FWM) .The frequency of the new optical field is given by [44]

$$\omega_4 = \omega_1 \pm \omega_2 \pm \omega_3 . \quad (2.5.3)$$

where ω_1 ω_2 ω_3 are the frequencies of the three original optical fields, and ω_4 is the

frequency of the new optical field. The "±" sign is relative to the energy transformation condition [45].

Unlike SPM and XPM, FWM is not dependent on bit rate; instead FWM depends on channel spacing and fiber dispersion. Since dispersion depends on the signal wavelength, the group velocities of the newly generated optical wave and reference signal wave are not identical. Phase matching is not possible if group velocities are different. Interference may occur when the new wave and original wave have the same wavelength which could decrease the new optical wave power. This decreases the signal to noise ratio (SNR) [44]. Table 2.3 represents a comparison of these three nonlinear refractive effects.

Table 2.3 Comparison of SPM, CPM and FWM

Nonlinear Effect	**SPM**	**CPM**	**FWM**
Bit rate	Dependent	Dependent	Independent
Origin	Nonlinear susceptibility	Nonlinear susceptibility	Nonlinear susceptibility
Effects	Phase shift due to pulse itself only	Phase shift is due to co-propagating pulses	New waves are generated
Shape of broadening	Symmetric	May be symmetric or asymmetric	N/A
Channel Spacing	No effect	Increases on decreasing the spacing	Increases on decreasing the spacing

In general, nonlinear effects degrade the performance of optical fiber communication by distorting the optical pulses. However, these effects provide gain to channels by increasing transmission rate at the expense of consuming power. SPM and CPM distort the signal phase and can also cause spectral broadening which results in dispersion. It is known that the nonlinear effects described above depend on transmission length and

optical intensity.

The fiber nonlinear effects are difficult to compensate for in high speed IM/DD systems. On the other hand, in digital coherent systems, the nonlinear effects can be mitigated by using the backward propagation methods based on solving the nonlinear Schrödinger equation and the Manakov equation [48] [49].

Besides nonlinear effects, one of the other major distortions in a fiber is laser phase noise.

2.6 Coherent Receiver

The detection method of optical coherent communication is coherent detection. Coherent detection relies on detecting a signal through a reference frequency carrier, commonly supplied by a local oscillator (LO) much more powerful than the signal.

Digital coherent receivers utilize a phase and polarization diverse architecture to map the optical field into the electrical domain. Once digitized, digital signal processing is used to track both the phase and polarization of the signal, which is much simpler to construct than optical homodyne receiver. The receiver maps the optical field into four electrical signals, which correspond to in-phase and quadrature field components (I and Q) for two polarizations [33].

In the coherent receiver, the optical signal is first mixed with a LO laser to down-convert the signal to microwave carrier frequency from optical carrier frequency. When the received signal is mixed with LO laser, an optical beat signal is generated at the photodiode, the frequency of which is equal to an intermediate frequency that is the frequency difference between the received signal and the LO laser. There are two types of coherent receivers. If the optical frequency of the signal is the same as that of the LO laser, the system is known as homodyne system. If the optical frequency of the signal differs from that of the LO laser, it is known as heterodyne system.

Homodyne system requires the local-oscillator frequency to be firmly locked in frequency and phase to the received signal and gives optimal receiver sensitivity [50]. The main constraint is that the frequency and phase of the local oscillator must be adjusted continuously. In order to deal with this problem, a phase-locked loop (PLL) is often used. On the other hand, a heterodyne system shows the advantage of relaxing the constraints on the linewidth of the lasers. Compared with homodyne detection, heterodyne system is easier to implement. However, heterodyne detection requires a higher receiver bandwidth [51]. Furthermore, the sensitivity of a heterodyne detector is normally worse than homodyne detection, which is due to the fact that effective energy of a heterodyne-detected signal is half of the signal effective energy of homodyne detection [52].

2.7 Digital Signal Processing Algorithms

In this thesis, we focus on PMD and polarization rotation effect as major effects in channel because POL-QAM and SP-QAM are both dual-polarization modulation. PMD effect, polarization rotation effect and laser phase noise effect could be compensated or equalized by utilizing corresponding carrier phase recovery algorithms. For PMD and polarization rotation equalization, least-mean square (LMS), zero-forcing(ZF), constant modulas algorithm (CMA) and multimodulus algorithm (MMA) are introduced. For laser phase noise recovery, Viterbi&Viterbi and decision directed (DD) carrier phase estimation algorithm are presented.

2.7.1 PMD and Polarization Rotation Equalization

In optical fiber communication, the inter-symbol interference (ISI) effect which caused by limited bandwidth or multi-path propagation, seriously degrades the performance of

optical fiber communication systems, limits data transmission speed, and increases the bit error rate (BER). ISI, PMD and polarization rotation effect obviously distort symbol demodulation at the receiver. Channel equalization is a normal technique to mitigate these effects and compensate for channel distortions. [53]

An equalizer is a filter which aims to estimate a general inverse of the optical channel response. Conventional equalization is a technique which utilizes a known training sequence. The coefficients of equalizer are adapted by applying adaptive algorithm such as LMS. Nevertheless, the throughput of the system decreases by the additional overhead of the transmitted signal when applying training sequence at the transmitter. In order to avoid utilizing the overhead, blind equalization (such as CMA or MMA) can be used to eliminate the need for training sequence. Blind equalization saves bandwidth, and improves the reliability of communication. [54]

Figure 2.11 shows a block diagram of equalization of dual-channel modulation.

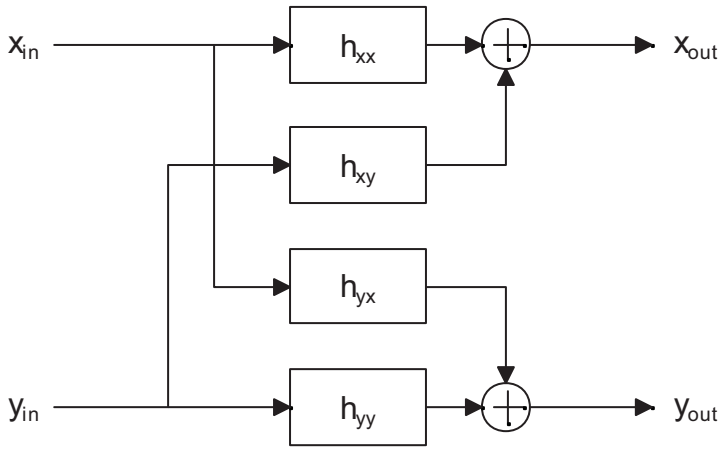

Figure 2.11 Equalization of dual-channel modulation

(1) **LMS adaptive equalization**

Least Mean Square (LMS) algorithm is an adaptive signal processing algorithm. The advantages of LMS are 1): Its simplicity of implementation; 2): Robust performance.

LMS is a stochastic algorithm and is based on training sequence to calculate the error function at each iteration.

An example of LMS algorithm for dual-channel optical transmission (such as PDM-QPSK) is shown as follows,

$$x_{out} = \mathbf{h}_{xx}^{H}\mathbf{x}_{in} + \mathbf{h}_{xy}^{H}\mathbf{y}_{in}, \qquad y_{out} = \mathbf{h}_{yx}^{H}\mathbf{x}_{in} + \mathbf{h}_{yy}^{H}\mathbf{y}_{in} \tag{2.7.1a}$$

where $\mathbf{h} = \begin{bmatrix} \mathbf{h}_{xx} & \mathbf{h}_{yx} \\ \mathbf{h}_{xy} & \mathbf{h}_{yy} \end{bmatrix}$ is an N-tap adaptive LMS filter, where the tap weights vector is adapted using the stochastic gradient algorithm:

$$\mathbf{h}_{xx} = \mathbf{h}_{xx} + \mu e_x \mathbf{x}_{in}, \tag{2.7.1b}$$

$$\mathbf{h}_{xy} = \mathbf{h}_{xy} + \mu e_x \mathbf{y}_{in}, \tag{2.7.1c}$$

$$\mathbf{h}_{yx} = \mathbf{h}_{yx} + \mu e_y \mathbf{x}_{in}, \tag{2.7.1d}$$

$$\mathbf{h}_{yy} = \mathbf{h}_{yy} + \mu e_y \mathbf{y}_{in} \tag{2.7.1e}$$

where the error term $e_x = D_x - \mathrm{x}_{out}$; $e_y = D_y - y_{out}$; D_x and D_y are training sequences. μ is the step-size parameter that controls the speed of convergence.

(2) **Zero-Forcing**

Zero-Forcing is an ideal algorithm to compensate for channel effects. It employs inverse Jones Matrix to compensate for PMD:

$$\mathrm{E}_{\mathrm{out\_PMD}}(t) = \mathbf{J} \bullet E_{in}(t) + \mathrm{n} \tag{2.7.1f}$$

$$\mathrm{E}_{\mathrm{out\_ZF}}(t) = \mathbf{J}^{-1} \bullet \left[\mathbf{J} \bullet E_{in}(t) + \mathrm{n}\right] = E_{in}(t) + \mathbf{J}^{-1} \bullet \mathrm{n} \tag{2.7.1g}$$

where n is coherent receiver noise, $\mathbf{J}$ is Jones matrix, $\mathbf{J}^{-1}$ is the inverse of Jones matrix. As shown above, ZF compensates for Jones matrix (PMD effect) at the expense of enhancing coherent receiver noise.

(3) **CMA adaptive equalization**

Constant modulus algorithm (CMA) is a well-known algorithm in optical communication systems as it does not require training sequence [55]. After Godard proposed CMA [56] in 1980, CMA has been commonly used for blind equalization. The CMA algorithm defines a cost function to estimate channel deviation in a received signal where the output value of the cost function is proportional to the channel deviation. The equalization algorithm first obtains an equalized signal by applying the outcomes of the received signal and the tap weights. Afterwards, the cost function calculates the output (cost) of the equalized signal. This cost function corresponds to the noise degree of the received signal. The equalizer then calculates a new equalized signal by utilizing the new error cost and received signal. By doing so, a new cost from the new equalized signal is produced and it is expected to be decreased by repeating the above procedure. The aim is to decrease the cost value and estimate an approximate channel coefficient [54]. The CMA equalizer is shown in Figure 2.12.

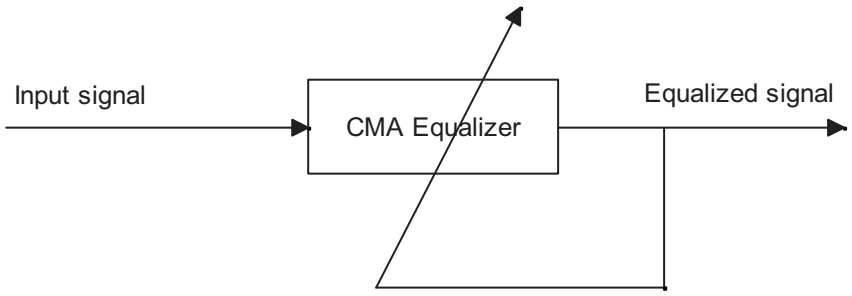

Figure 2.12 Schematic of CMA equalizer

Assuming PDM-QPSK, normalizing the envelope of each polarization signal to 1, the

CMA becomes dual-polarization CMA (DP-CMA). Similar to the LMS filter, the output is given by (2.7.1a), with changes to the error term and the stochastic gradient algorithm:

$$\mathbf{h}_{xx} = \mathbf{h}_{xx} + \mu e_x \mathbf{x}_{in} x_{out}^*, \quad (2.7.1h)$$

$$\mathbf{h}_{xy} = \mathbf{h}_{xy} + \mu e_x \mathbf{y}_{in} x_{out}^*, \quad (2.7.1i)$$

$$\mathbf{h}_{yx} = \mathbf{h}_{yx} + \mu e_y \mathbf{x}_{in} y_{out}^*, \quad (2.7.1j)$$

$$\mathbf{h}_{yy} = \mathbf{h}_{yy} + \mu e_y \mathbf{y}_{in} y_{out}^* \quad (2.7.1k)$$

with error $e_x = 1 - \left|x_{out}\right|^2$; $e_y = 1 - \left|y_{out}\right|^2$. It is shown that CMA is based on the principle of minimizing the modulus variation of the output signal to update its weight vector.

(4) **MMA adaptive equalization**

CMA becomes a popular equalization algorithm due to its LMS-like complexity and ideal robustness performance. However, the disadvantage of CMA is its independent convergence of carrier recovery which may result in a phase error to output constellation. Due to this fact, a rotator needs to be added at the output of equalizer which may increase the complexity of receiver implementation. A multi-modulus algorithm (MMA) has been proposed in order to improve the drawback of CMA [57]. The MMA does not need a rotator at the output of the equalizer in steady-state operation. [58] The algorithm is works as follows:

$$\mathbf{h}_{xx} = \mathbf{h}_{xx} + \mu e_x^* \mathbf{x}_{in}, \quad (2.7.1l)$$

$$\mathbf{h}_{xy} = \mathbf{h}_{xy} + \mu e_x^* \mathbf{y}_{in}, \quad (2.7.1m)$$

$$\mathbf{h}_{yx} = \mathbf{h}_{yx} + \mu e_y^* \mathbf{x}_{in}, \quad (2.7.1n)$$

$$\mathbf{h}_{yy} = \mathbf{h}_{yy} + \mu e_y^* \mathbf{y}_{in} \quad (2.7.1o)$$

with error $e_x = x_{out\_R} \times (\mathrm{R}_{x\_R} - |x_{out\_R}|^2) + j \cdot x_{out\_I} \times (\mathrm{R}_{x\_I} - |x_{out\_I}|^2)$; $e_y = y_{out\_R} \times (\mathrm{R}_{y\_R} - |y_{out\_R}|^2) + j \cdot y_{out\_I} \times (\mathrm{R}_{y\_I} - |y_{out\_I}|^2)$, where x_{out_R} is the real value of the output in the x-polarization; x_{out_I} is the imaginary value of the output in the x-polarization; y_{out_R} is the real value of the output in y-polarization; y_{out_I} is the imaginary value of the output in the y-polarization. R_{x_R} is the real part of the estimate of the signal envelope in the x-polarization; R_{x_I} is the imaginary part of the estimate of the signal envelope in the x-polarization; R_{y_R} is the real part of the estimate of the signal envelope in the y-polarization; R_{y_I} is the imaginary part of the estimate of the signal envelope in the y-polarization.

2.7.2 Carrier phase recovery

In this section, we present carrier phase estimation algorithms which are used to compensate for laser phase noise effect.

(1) **Viterbi &Viterbi carrier phase estimation algorithm**

Viterbi&Viterbi (V&V) Algorithm is a carrier phase recovery algorithm, which is able to compensate for laser phase noise and even nonlinear optical phase distortion in normal QPSK signals.

V&V is a non-data-aided (NDA) feed-forward carrier phase estimation algorithm [43]. The following equation explains this algorithm:

$$\mathrm{X}_k = A_k \exp(j\theta_k + j\phi_k + j\phi_k^{NL}) + n \quad (2.7.2a)$$

where X_k is the input signal, ϕ_k is the carrier phase of the signal, ϕ_k^{NL} is nonlinear phase distortion and noise. The estimate of phase noise is calculated as follows:

$$\hat{\phi}(k) = \frac{1}{M} \arg[\sum_{j=-N}^{N} X_{k+j}^{M} \cdot e^{-j\pi}] \tag{2.7.2b}$$

For simplicity, 4-ary modulation format (such as QPSK), *M*=4 is used. As seen from (2.7.2b), the signal first raised to M-th power and minus pi in phase in order to eliminate the phase modulation. Then average the calculated signal over 2*N*+1 samples to improve the SNR of the estimated phase reference [7].The estimated phase is obtained by dividing by *M*. Then the obtained phase has the ambiguity by 2π/*M*. Phase unwarping (shown in Figure 2.12) is necessary to implement. The phase unwarping rule is described as follows:

$$\theta_e(i) = \theta_e(i) + \frac{2\pi}{M} f(\theta_e(i) - \theta_e(i-1)) \tag{2.7.2c}$$

where f(x) is

$$f(x) = \begin{cases} +1 \; if \; x < -\pi / M \\ 0 \quad if \; |x| \le \pi / M \\ -1 \; if \; x > \pi / M \end{cases} \tag{2.7.2d}$$

Figure 2.13 shows an example of phase unwarpping.

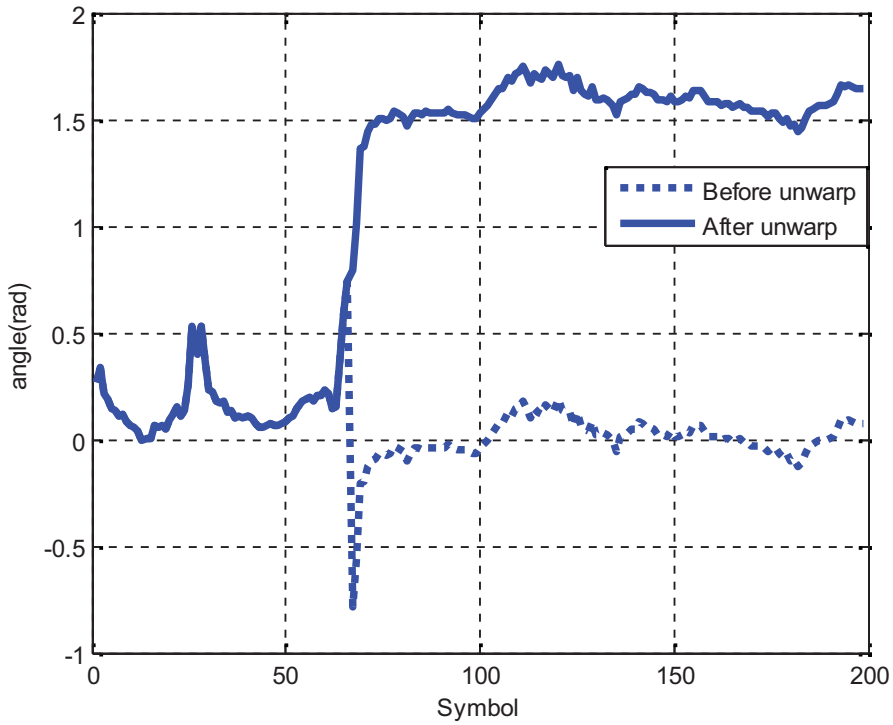

Figure 2.13 Phase unwrapping

Finally the output phase is acquired from the input phase as shown in (2.7.2e).

$$X_{k,out} = X_k \cdot e^{-j\hat{\phi}(k)} \tag{2.7.2e}$$

Figure 2.14 shows a block diagram of the Viterbi&Viterbi algorithm.

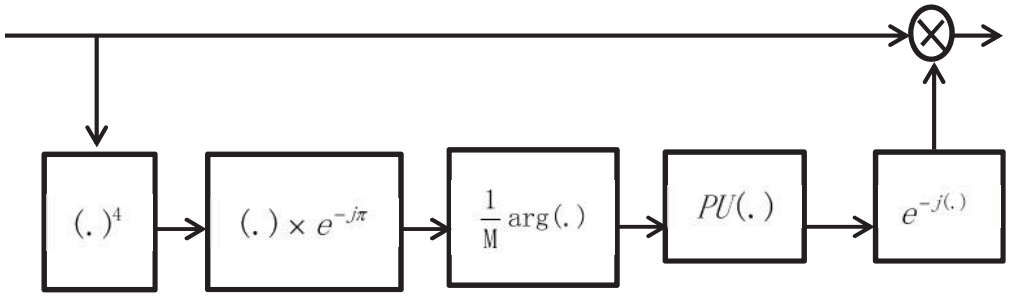

Figure 2.14 Block diagram of Viterbi&Viterbi phase recovery algorithm

(2) **Decision-directed carrier phase recovery algorithm**

For M-QAM (M>4) systems, it is not suitable to use V&V to recover the carrier phase information, instead decision-directed (DD) carrier phase recovery algorithm is investigated. The DD carrier phase recovery loop error is calculated by using the output of the equalizer and the decision at the output [55]. The phase update is described by:

$$\hat{\phi}(k+1) = \hat{\phi}(k) - \mu_{\phi}\,\mathrm{Im}[z(k)e^{*}(k)] \qquad (2.7.2f)$$

Figure 2.15 shows the block diagram of the combined blind equalization and DD carrier phase recovery.

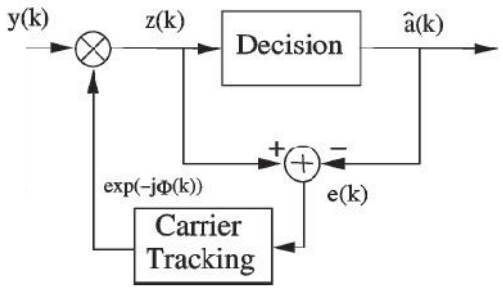

Figure 2.15 Block diagram of DD carrier phase recovery algorithm [55]

In (2.7.2f), μ_{ϕ} is the step size and $e(k)$ is the DD error, which is described as:

$$e(k) = z(k) - \hat{a}(k) \qquad (2.7.2g)$$

with $\hat{a}(k)$ as the decision of the equalized signal.

2.8 Conclusions

In this chapter, we provided an overview of optical transmission system model. An introduction of a fiber link through transmitter to receiver is given. In particular, we showed the structure of the transmitter, using new modulation formats. Furthermore, we introduced different effects of distortion occur in the fiber link, such as PMD and polarization effect. To compensate for these effects, various digital signal processing algorithms are introduced, such as equalization algorithms and carrier phase estimation algorithms.

Chapter 3

Equalization of POL-QAM and SP-QAM

3.1 Introduction

In this chapter, the performance of POL-QAM and set-partitioning QAM (SP-QAM) with our modified CMA equalization and MMA equalization are investigated. Through our investigating, it is noted that the conventional CMA equalization algorithm is not suitable for POL-QAM. This motivates us to introduce a modified CMA algorithm which is shown to perform better than the conventional CMA. In this chapter, we also study the channel effects on POL-QAM transmission.

In optical coherent communication, polarization mode dispersion (PMD) distorts the pulse width and results in power penalty at the receiver, which is considered a significant issue for the transmission performance in fiber channel. In order to compensate for the distortion caused by PMD and polarization rotation effects (discussed in chapter 2), channel equalization has been integrated in digital signal processing. The channel (PMD and fiber polarization rotation effects) can be measured as a function of wavelength and time by using the Jones matrix [59].

3.1.1 Prior Work

Henning Bülow introduced POL-QAM in 2009 [23], where both exhaustive constellation architecture and modulator architecture for POL-QAM are discussed. By their new achievement, they increased two state-of–polarizations (SOPs) of the polarization division multiplexed QPSK (PDM-QPSK) constellation. The additional two SOPs result in a split-new modulation format POL-QAM 6-4 without altering minimal Euclidean distance. For this new modulation format, i.e. POL-QAM 6-4, the spectral efficiency is increased by 14% compared to PDM-QPSK. Furthermore, one additional bit is added for every two symbols (9 bits for POL-QAM 6-4 compared with 8 bits for PDM-QPSK), which enables us to apply an inner Reed-Solomon (511,455) code to POL-QAM 6-4. Henning Bülow also compared the BER performance of un-coded POL-QAM with encoded POL-QAM using 5-tap fractionally spaced complex butterfly FIR (LMS filter) and a 5th order low pass Bessel filter. It has been shown in [23] that an improvement in sensitivity of 1.7dB can be achieved when using RS(511,455) encoded POL-QAM 6-4 compared to PDM-QPSK.

In addition, more spectrally efficient 4D formats such as 128 SP-QAM (presented in chapter 2) has been proposed recently [37]. Due to its long transmission distance compared to PDM-16QAM, the performance of 128 SP-QAM has been studied using LMS equalization and carrier phase recovery without considering PMD effects [38]. To fill this void, in this thesis, we investigate the performance of 128 SP-QAM in long-haul systems considering channel effects.

3.2 System Model

Consider an optical coherent communication system where, 112Gbits/s Dual-Polarization (DP) modulation format such as POL-QAM and SP-QAM has been used to modulate the signal at the transmitter. The laser wavelength is 1550nm. The DP-modulation which is

commonly transmitted on two orthogonal linear polarizations (x and y), is known to be sensitive to PDM effect and the polarization rotation in the fiber channel. In this thesis, POL-CMA, MMA and LMS are chosen to equalize the received signal in the DSP part of the receiver. Figure 3.1 shows the system model used in this chapter.

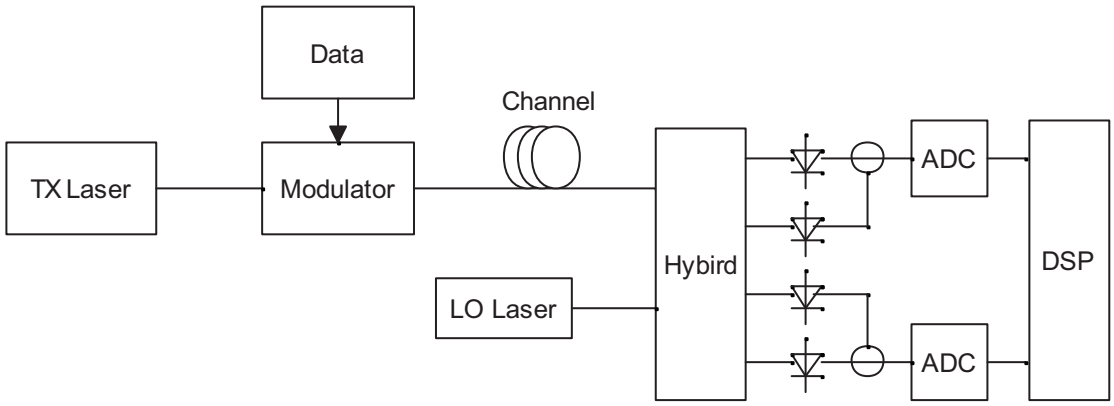

Figure 3.1 Optical system model

The corresponding sampled received baseband signal is given by

$$y = e^{-\alpha L} \cdot \mathrm{J} \cdot x + \mathrm{n} \tag{3.2.1}$$

where y is the $2\times N$ received signal (in two polarizations) after coherent part, N is the equalizer tap length, α is the attenuation factor of the fiber, L is the fiber length (km). J is the 2×2 channel matrix (in this thesis, channel effect are expressed as Jones matrix), x is the $2\times N$ transmitted signal, n is the noise vector at the coherent receiver which is modeled as Gaussian distributed in the corresponding channel bandwidth, the variance of the coherent receiver noise is presented in [60] as follows:

$$\delta_n^2 = 2eR_p \frac{P_{L0}}{2}\frac{B}{2} + 4eR_p \frac{\eta(G-1)n_{SP}}{2}\frac{P_{L0}}{2}\frac{B}{2} + \frac{4kT}{R_{in}}\frac{B}{2} \tag{3.2.2}$$

where e is the electron charge, R_P is the responsivity of photodiodes, P_{LO} is the power of local oscillator, B is the bandwidth of the coherent receiver, η is the quantum efficiency of photodiodes, G is the preamplifier gain, n_{SP} is the spontaneous emission factor of the preamplifier, and kT is the thermal energy for the double-balanced photodiodes [60].

3.3 POL-CMA for POL-QAM

CMA is a blind equalization algorithm which eliminates the need for the training overhead (presented in chapter 2). Dual polarization CMA (DP-CMA) has been used for dual polarization equalization [61]. In this thesis, our focus will be on dual- polarization modulation formats such as PDM-QPSK, SP-QAM. As mentioned earlier, DP-CMA is not suitable for POL-QAM due to the fact that it equalizes two polarizations separately, which is suitable for conventional modulation formats (PDM-16QAM, PDM-4QAM). Since POL-QAM 6-4 is based on joint modulation of signals, conventional DP-CMA cannot be used to equalize POL-QAM 6-4.

For this reason, we propose a modified CMA (named POL-CMA), which compares the power of each output polarization from the equalizer. There are three levels of output power in POL-QAM 6-4 modulation which are normalized to 0, 2 and 4. The modified CMA algorithm works as follows

Step 1: Calculate the value of $\left\| X_{out} \right| - \left| Y_{out} \right\|$,

Step 2: If $\left\| X_{out} \right| - \left| Y_{out} \right\| < 1$, the CMA goes to a DP-CMA mode [61], $R_x = R_y = 2$; If not, go to step 3.

Step 3: If $|x_{out}| > |y_{out}|$,

R_x=4; R_y=0,

else

R_x=0; R_y=4,

End

where x_{out} and y_{out} are outputs of the equalizer on x and y polarizations, R_x and R_y represent imaginary modulus in each polarization, which issued to calculate the error.

$$e_x = R_x - |x_{out}|^2; e_y = R_y - |y_{out}|^2 \quad (3.3a)$$

The values of the equalizer taps are given by:

$$\mathbf{h}_{xx} = \mathbf{h}_{xx} + \mu e_x \mathbf{x}_{in} x_{out}^*, \quad (3.3b)$$

$$\mathbf{h}_{xy} = \mathbf{h}_{xy} + \mu e_x \mathbf{y}_{in} x_{out}^*, \quad (3.3c)$$

$$\mathbf{h}_{yx} = \mathbf{h}_{yx} + \mu e_y \mathbf{x}_{in} y_{out}^*, \quad (3.3d)$$

$$\mathbf{h}_{yy} = \mathbf{h}_{yy} + \mu e_y \mathbf{y}_{in} y_{out}^* \quad (3.3e)$$

where $\mathbf{h} = \begin{bmatrix} \mathbf{h}_{xx} & \mathbf{h}_{yx} \\ \mathbf{h}_{xy} & \mathbf{h}_{yy} \end{bmatrix}$ is adaptive equalizer coefficient.

$$x_{out} = \mathbf{h}_{xx}^H \mathbf{x}_{in} + \mathbf{h}_{xy}^H \mathbf{y}_{in}, \quad (3.3f)$$

$$y_{out} = \mathbf{h}_{yx}^H \mathbf{x}_{in} + \mathbf{h}_{yy}^H \mathbf{y}_{in} \quad (3.3g)$$

where $\mathbf{x}_{in}$ and $\mathbf{y}_{in}$ are input vectors in two polarizations.

As described above, the proposed POL-CMA equalization algorithm is a “variable” modulus algorithm where a decision circuit is used to decide on the adaptive error calculation mode. Figure 3.2 shows a block diagram of such an equalizer where the equalizer calculates x_{out} and y_{out} using (3.3f)-(3.3g).

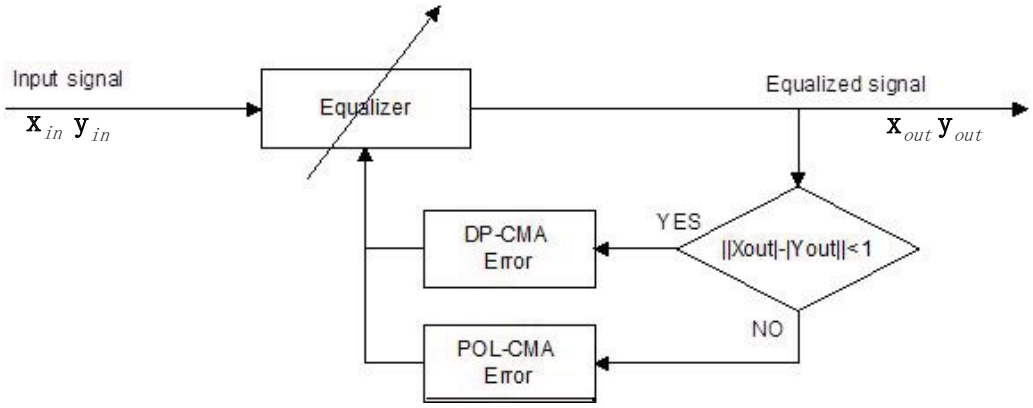

Figure 3.2 Block diagram of POL-CMA architecture

3.4 Simulation Results

In this section, simulation results are provided to show the accuracy of our proposed algorithm. In the simulation, POL-QAM 6-4 and 128-SP-QAM are used as dual-polarization modulation formats at the transmitter. We investigate the performance of the two modulations considering channel effects using our proposed equalization algorithms.

3.4.1 Equalization of POL-QAM 6-4

In figure 3.3, we simulated 112Gb/s POL-QAM 6-4. Attenuation factor α =0.165dB/km and fiber length L=480km, the step size of POL-CMA is optimized which will be discussed later and the tap length N=7. It is shown that the signal is distorted by PMD and polarization effect in the channel with both amplitude and phase variation. After coherent detection, we can see the POL-CMA well compensates for the channel effect and recovers the distorted signal.

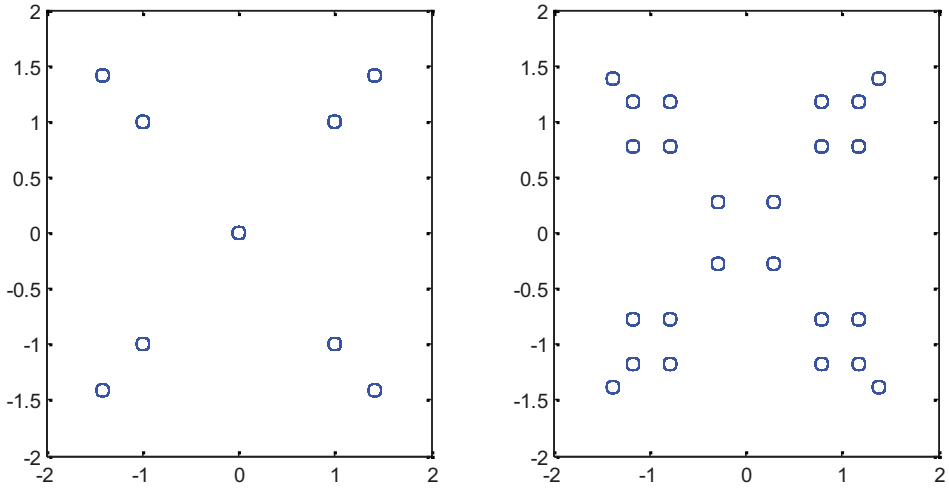

(a) (b)

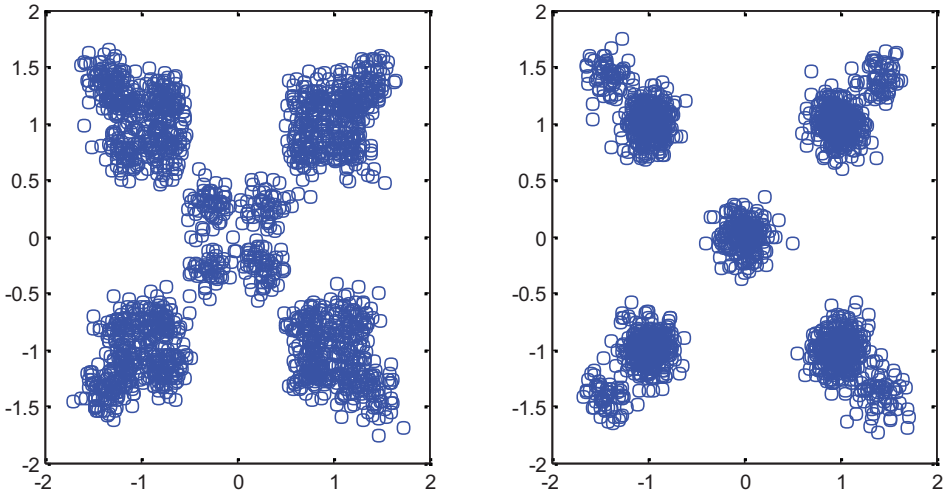

(c) (d)

Figure 3.3 POL-QAM 6-4 constellation change during equalizing: (a) X-polarization constellation of POL-QAM 6-4 at transmitter; (b) X-polarization constellation of POL-QAM 6-4 after the channel; (c) X-polarization constellation of POL-QAM 6-4 after coherent receiver; (d) Compensated by POL-CMA

Figure 3.4 depicts the BER performance of POL-QAM 6-4 for different step size of POL-CMA and LMS. For the LMS algorithm, we employ a training sequence of 2000 symbols in every 4000 symbols as an overhead. From these results, it shown that when the POL-CMA and LMS are employed, the step size of the adaptive algorithm clearly affects the performance of equalization. Through simulations, the optimal step size of 7-tap POL-CMA and LMS for POL-QAM 6-4 is set to $\mu_{CMA}=\mu_{LMS}=10^{-3}$. We use the optimal step size for the rest of our simulations.

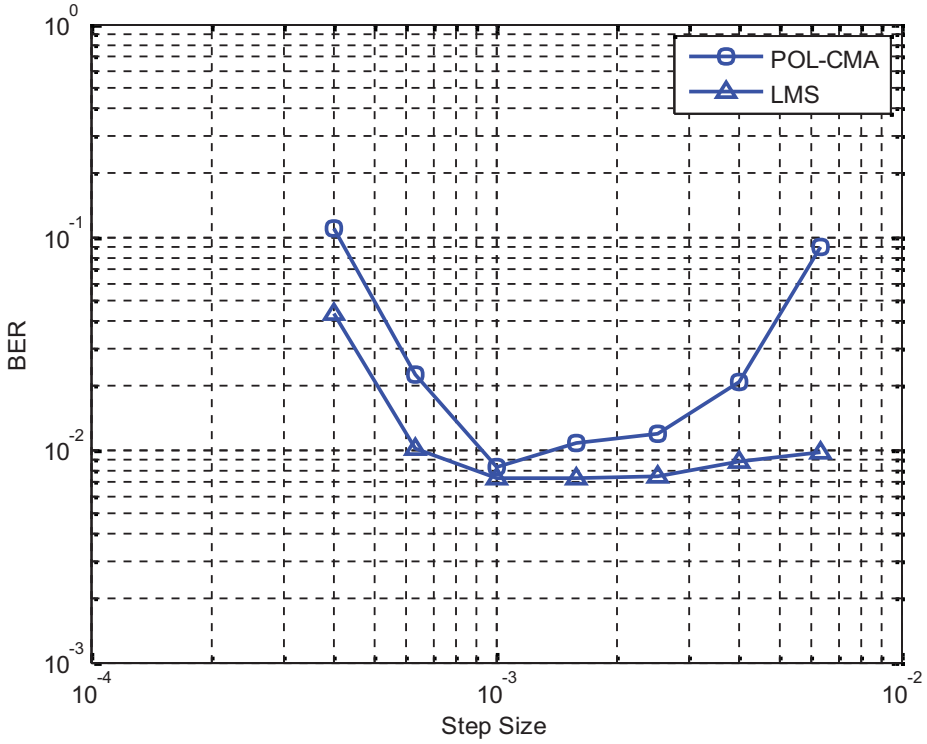

Figure 3.4 POL-QAM BER with step size of POL-CMA and LMS

In Figure 3.5, the simulation of Mean Square Error (MSE) of POL-CMA for POL-QAM 6-4 is been provided. For the calculation of MSE [62],

$$MSE = \frac{1}{n}\sum_{i=1}^{n}(\hat{Y}_i - Y_i)^2 \tag{3.4.1}$$

where n is number of estimated symbols, $\hat{Y}$ is the prediction of the signal symbol, and Y is the original value [62]. In this simulation, L=340km. As we can see, POL-CMA provides faster convergence than LMS. POL-CMA reaches a convergence after 1000 symbols; LMS reaches a convergence after 1600 symbols.

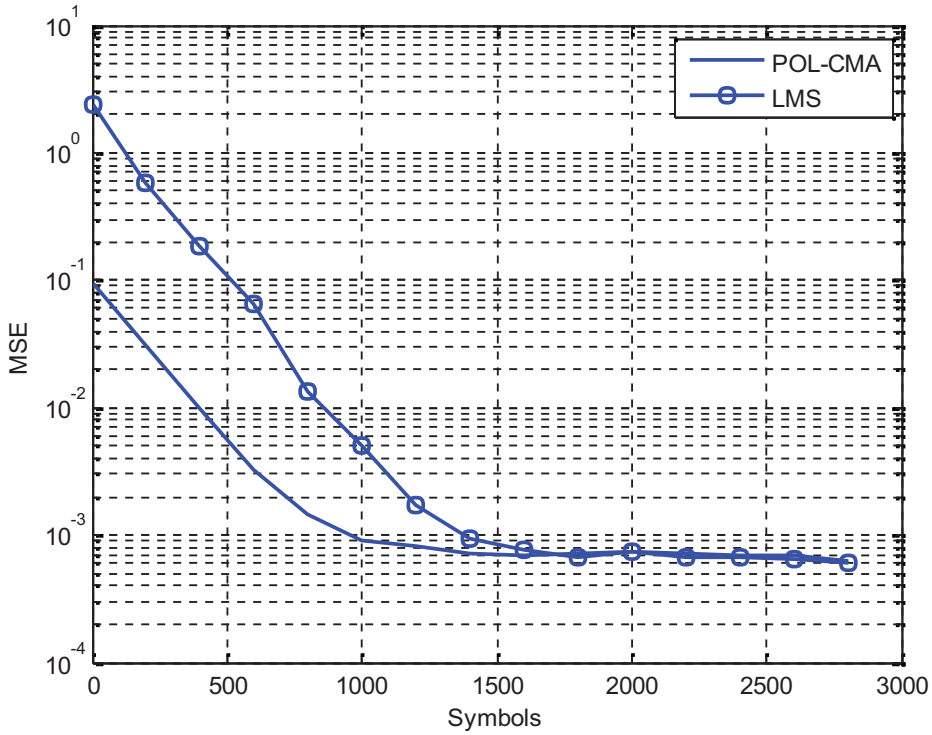

Figure 3.5 Mean Square Error of POL-CMA for POL-QAM

Figure 3.6 compares the BER performance of equalization algorithms for POL-QAM 6-4 and PDM-4QAM as a function of the fiber length. As shown, POL-CMA and LMS have almost similar performance for POL-QAM 6-4. POL-CMA has the advantage of blind equalization without losing much sensitivity. From this figure, we can see that PDM-4QAM outperforms un-coded POL-QAM 6-4. To improve the POL-QAM 6-4 performance, we employed Reed-Solomon code to this modulation which will be discussed in Chapter 4.

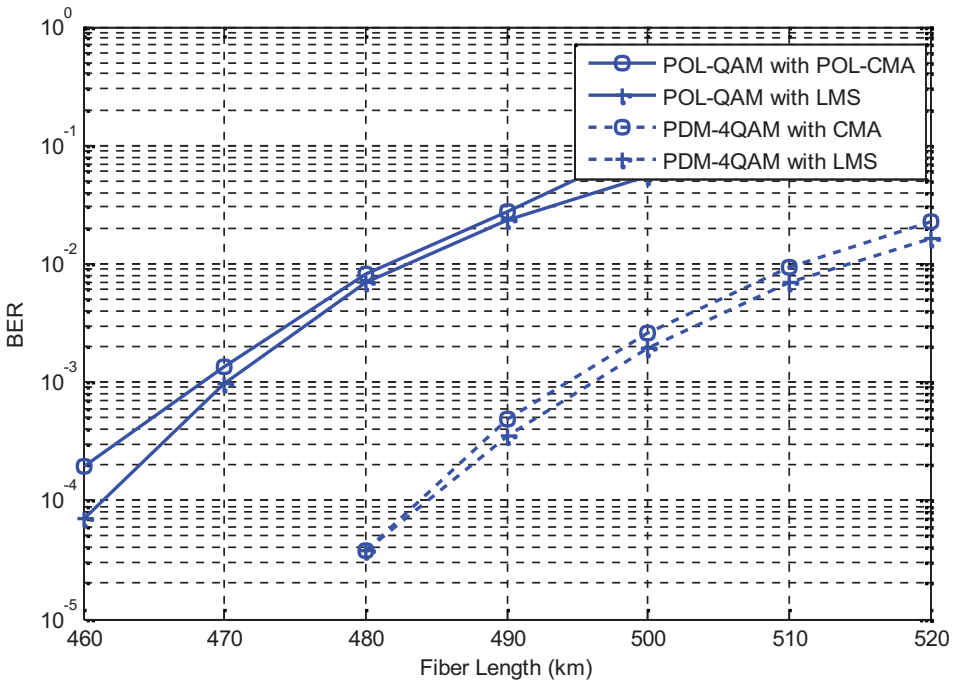

Figure 3.6 BER performance of POL-QAM 6-4 with POL-CMA and LMS

3.4.2 Equalization of SP-QAM

In this section, we investigate the performance of 128-SP-QAM considering fiber channel effects. As described in chapter 2, due to the fact that 128-SP QAM and PDM-16QAM are both modulation formats with non-constant modulus, conventional CMA equalization cannot be used since it is used to equalize constant modulus modulation formats. To overcome this problem, MMA is used to equalize multi-modulus modulation formats such as 128-SP-QAM and PDM-16QAM.

In Figure 3.7, non-differential coding 128-SP-QAM has been simulated. These results are based on fiber length L=455km, and an optimized step size of 7-tap POL-CMA. As seen, the constellation is similar to PDM-16QAM where an MMA equalizer is used to compensate for the channel instead of CMA equalization.

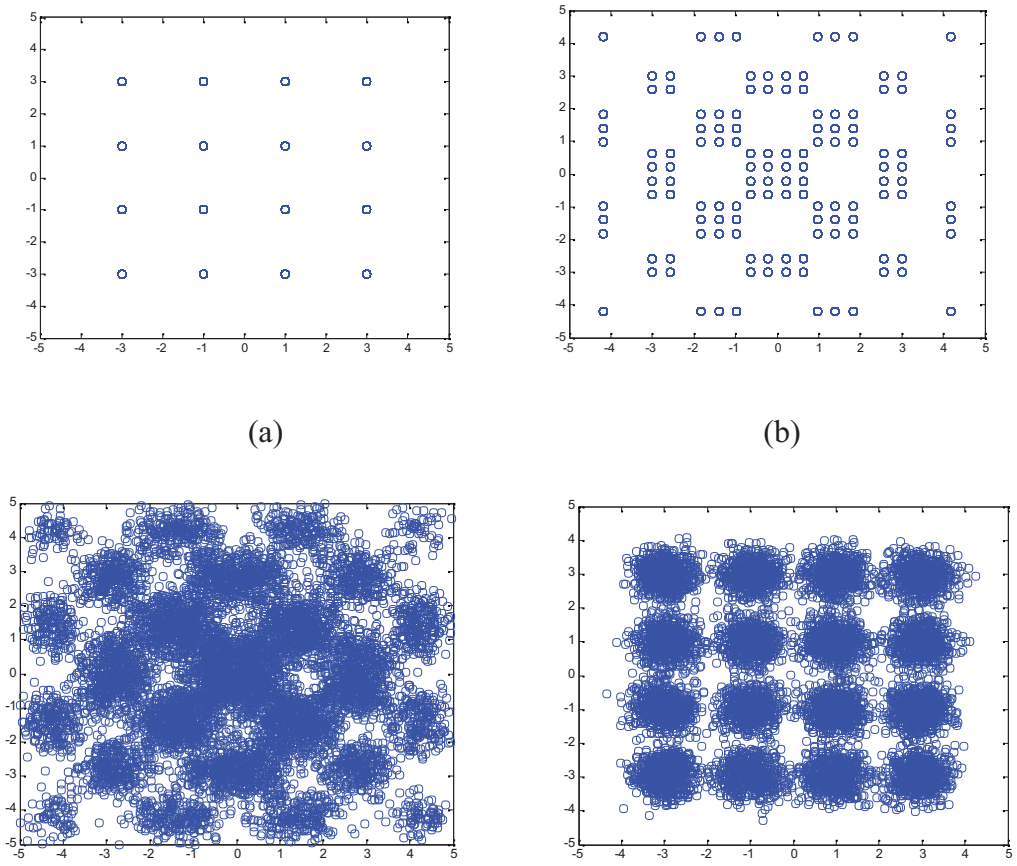

(a) (b)

(c) (d)

Figure 3.7 128-SP-QAM constellation change during equalizing (a) X-polarization constellation of 128-SP-QAM at transmitter; (b) X-polarization constellation of 128-SP-QAM after channel effect; (c) X-polarization constellation of 128-SP-QAM after coherent receiver; (d) Compensated by MMA

Figure 3.8 shows the BER performance of both MMA and LMS for 128-SP-QAM as a function of the step size using a fiber length L=465km.

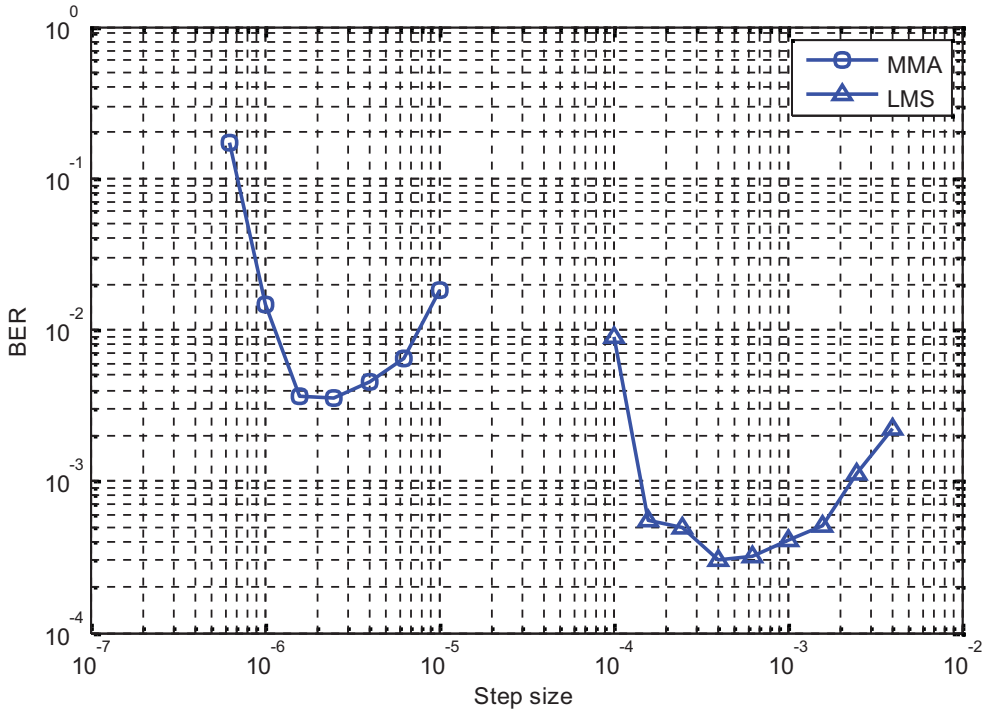

Figure 3.8 128-SP-QAM BER for MMA and LMS

Figure 3.9 shows the MSE of MMA and LMS for 128-SP-QAM. *L*=300km. MMA reaches a convergence after 1300 symbols; LMS reaches a convergence after 1600 symbols.

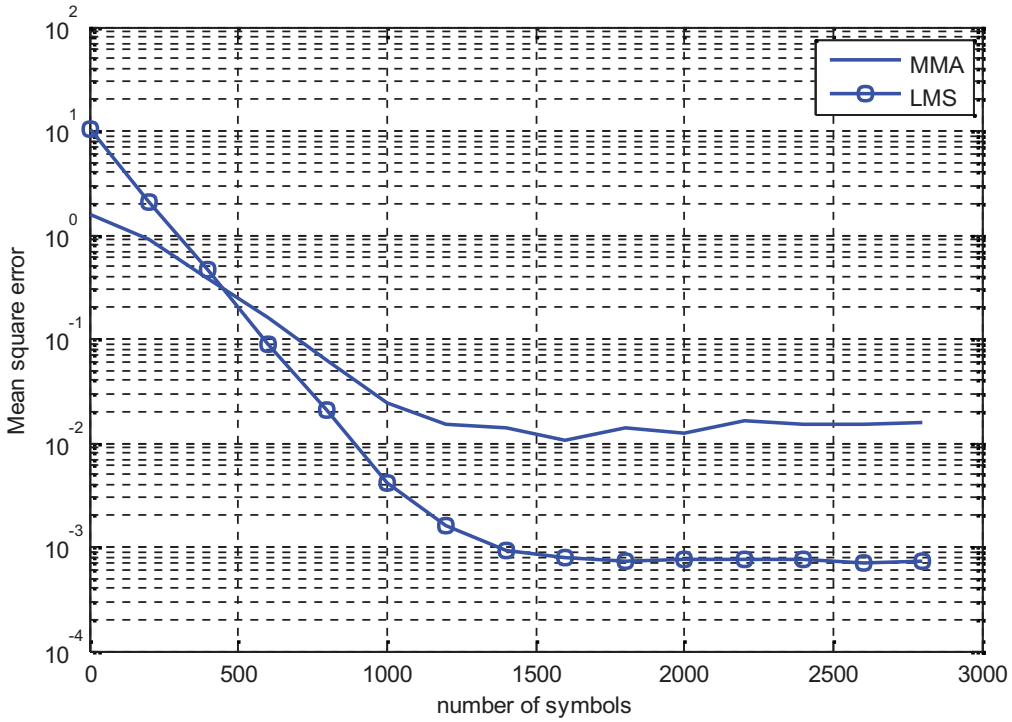

Figure 3.9 Mean Square Error (MSE) of MMA for 128-SP-QAM

Figure 3.10 shows the BER performance of 128-SP-QAM for different fiber lengths where MMA equalization is shown to offer less improvement compared with LMS equalization. This is due to the fact that MMA is a blind algorithm and hence some loss in performance relative to training based LMS equalization algorithm.

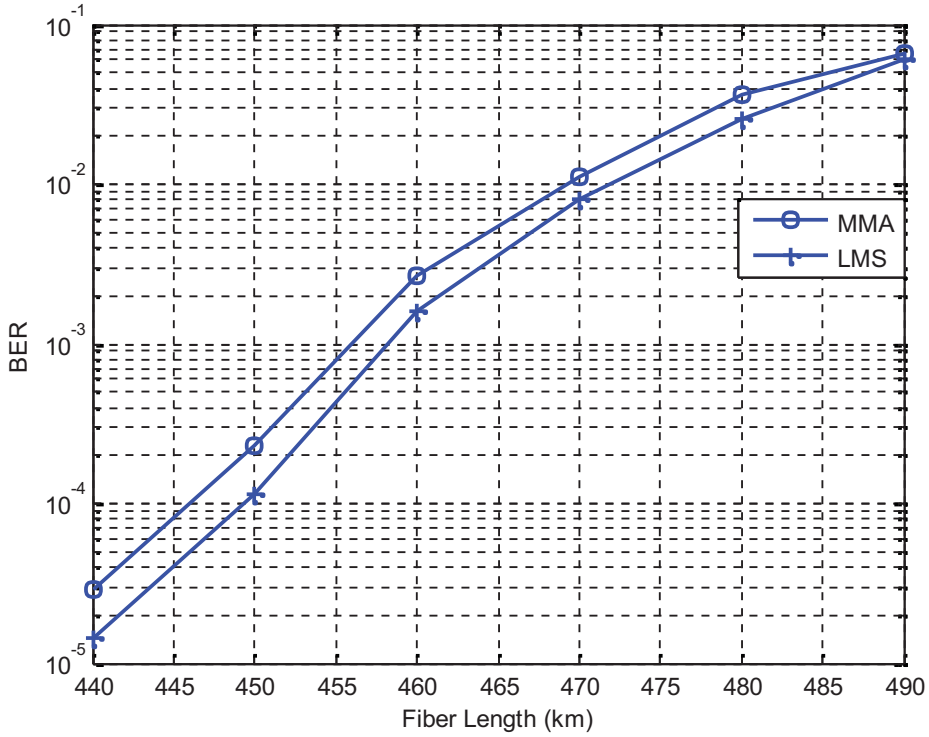

Figure 3.10 BER Performance of 128-SP-QAM as a function of fiber length

Figure 3.11 shows a performance comparison between 128-SP-QAM and PDM-16QAM when using MMA equalization. 128-SP-QAM shows better performance due to the fact that 128-SP-QAM employs non-differential coding, hence better transmission range (about 8km at BER 10^{-3}).

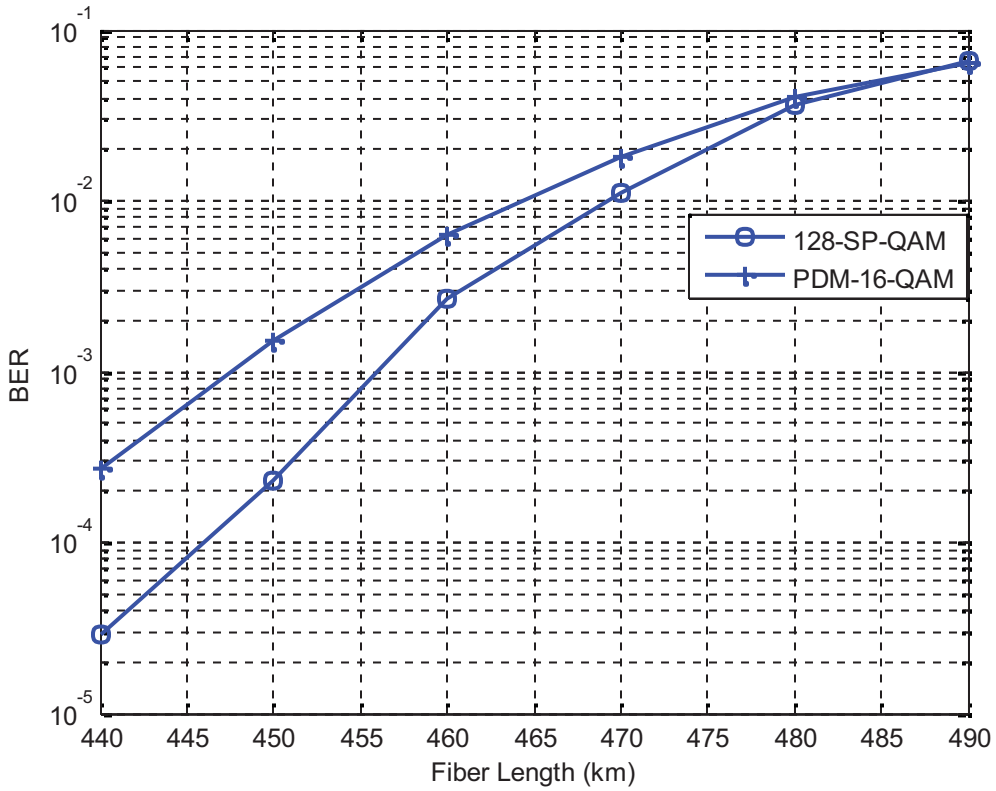

Figure 3.11 BER Performance of 128-SP-QAM and PDM-16-QAM with variable fiber length equalized by MMA

3.5 Conclusion

In this chapter, we proposed a new modified CMA to equalize POL-QAM signals. The POL-QAM is shown to well compensate for the channel PMD and polarization rotation effects. For SP-QAM modulation format, we used an MMA algorithm to equalize the signal and compare the simulation results to LMS. It is shown that LMS offers better BER performance compared to blind equalization algorithms such as POL-CMA or MMA. For the SP-QAM system, it is shown that 128-SP-QAM offers larger transmission range than PDM-16-QAM with the same QoS (i.e. BER). In the following chapter, to complete our study, carrier phase estimation algorithms for POL-QAM and SP-QAM will

be discussed.

Chapter 4

Performance in Long-Haul Transmission Systems

4.1 Introduction

In chapter 3, we discussed the high level modulation with different equalization algorithms at the receiver. We only took into account the fiber channel effect in the system model. In this chapter, we consider laser phase noise and Erbium Doped Fiber Amplifier (EDFA) effects in the transmission system and discuss their effects on our proposed algorithm (POL-CMA).

EDFA is a technology which used to amplify the optical signal in long-haul transmission systems. However, this signal amplification comes at the expense of producing amplifier noise which in turn degrades the performance of coherent receivers. The degree of the degradation is proportional to the number of amplifiers in the system. Overall, amplifier noise and laser phase noise are the main sources of distortion in the modern long-haul optical communication systems.

In this chapter, we first show through simulations the performance of POL-QAM 6-4 and 128-SP-QAM under laser phase noise effect. Then to compensate for phase noise,

Viterbi&Viterbi (V&V) and Decision Directed (DD) carrier phase estimation algorithms, discussed in section 2.7.2, are chosen for carrier phase recovery. Furthermore, we study the performances of the two modulation formats in long-haul transmission system, which employs optical amplifiers to compensate for the fiber attenuation loss.

4.2 Erbium Doped Fiber Amplifier

In late 1980s, Erbium Doped Fiber Amplifier was first invented as an optical amplifier and drew great attention [63]. It provides a totally new invention to optical fiber window centered at 1550nm and made it possible for long-haul optical transmission with high data rates. In a real optical transmission system, the amplified signal can be transmitted over 60km to 100km before further amplification. Figure 4.1 shows a schematic diagram of EDFA.

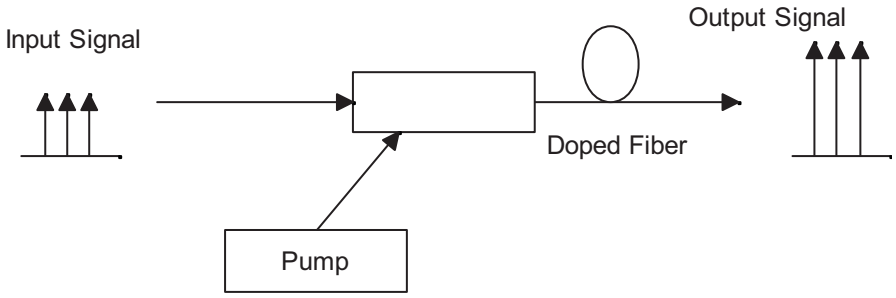

Figure 4.1 Schematic diagram of EDFA

Equation (4.2) represents the input-output relationship of the EDFA in fiber systems.

$$Y_{out} = G \cdot X_{in} + n_{EDFA} \tag{4.2}$$

where Y_{out} is the output signal after EDFA, G is the amplifier gain，which is defined as the ratio between the output and the input signal power of the amplifier [25], X_{in} is

the input signal of the amplifier, and n_{EDFA} is the noise induced by the EDFA.

4.2.1 EDFA Noise

In general all amplifiers cannot enhance the optical signal without distortion. This distortion is mainly caused by the amplified spontaneous emission (ASE) which results in noise during amplification [20]. The amplifier noise figure F_n is used to describe the ASE noise. [20]

$$F_n = \frac{SNR_{in}}{SNR_{out}} \tag{4.2.1a}$$

where SNR_{in} and SNR_{out} refer to the signal to noise ratio before and after amplification.

The spectral density of the ASE noise is given by:

$$\sigma^2 = n_{SP} h\nu_0 (G - 1) \tag{4.2.1b}$$

where h is Planck's constant equal 6.63×10^{-34}, ν_0 is the carrier frequency, G is the amplifier gain, n_{SP} refers to the spontaneous emission factor given by:

$$n_{SP} = \frac{\sigma_e N_2}{\sigma_e N_2 - \sigma_a N_1} \tag{4.2.1c}$$

with N_1 being the atomic population of the ground, N_2 is atomic population of the excited

states. In our simulations, n_{SP} is set to 1.41 [64].

4.3 System Model

Here we consider POL-QAM and SP-QAM to modulate the signal at the transmitter. The differences between the system model of chapter 3 and the one introduced here are as follows:

(1) Laser phase noise is considered.

(2) Optical amplifiers (EDFA) are used to increase the system transmission range.

In the DSP part, POL-CMA, MMA or LMS is chosen to equalize the received signal. For phase offset compensation, V&V and DD carrier phase estimation algorithms are used and compared (as described in chapter 2). Figure 4.2 shows the architecture of the underlying system.

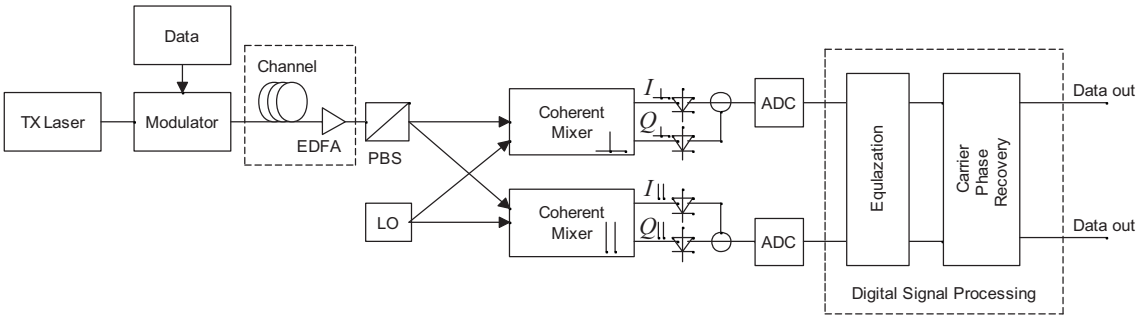

Figure 4.2 Architecture of long-haul system model

4.4 Simulation Results

In this section, we first analyze the performance of the high level modulation schemes under laser phase noise effects as the main distortion. Then, we present simulation results for POL-QAM 6-4 and 128-SP-QAM in long-haul systems separately.

4.4.1 Effect of Laser Phase Noise

As discussed in chapter 2, laser phase noise is a crucial impairment in the coherent optical communication system. In this section, we simulate POL-QAM 6-4 and 128-SP-QAM fiber communication systems with laser phase noise effect. Figure 4.3 (a)-(h) shows an example of the constellation for POL-QAM 6-4. The block length of the V&V algorithm $W_{v\&v}$=10 and the step size of the DD algorithm (discussed in section 2.7.2) μ_{DD} = 0.006, the fiber length L=400km, the bit rate R=112Gbit/s, the laser linewidth $\Delta\nu$ =1000kHz, and the fiber attenuation factor α =0.165dB/km. Figure 4.3 (a)(b) show the original constellations of POL-QAM 6-4 before transmission. (c)(d) show the phase offset effect on the optical system. (e)(f) show the effect of receiver noise. As we can see from Figure 4.3 (g)(h), the V&V compensates for the phase offset and recovers the noise-induced signal.

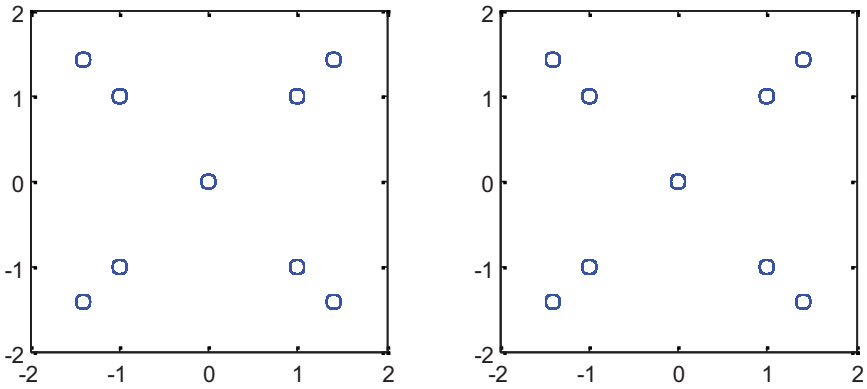

(a) POL-QAM 6-4 x-polarization (b) POL-QAM 6-4 y-polarization

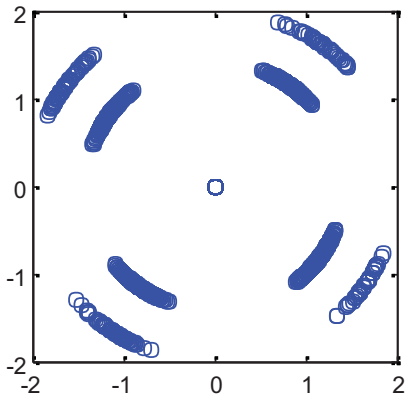

(c) x-polarization under phase offset

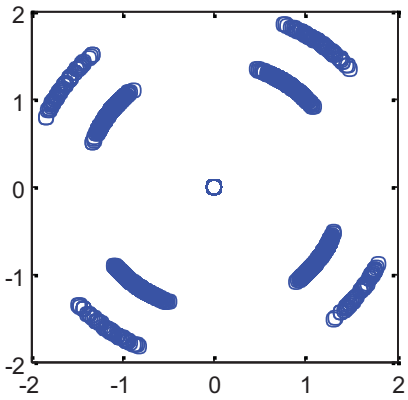

(d) y-polarization under phase offset

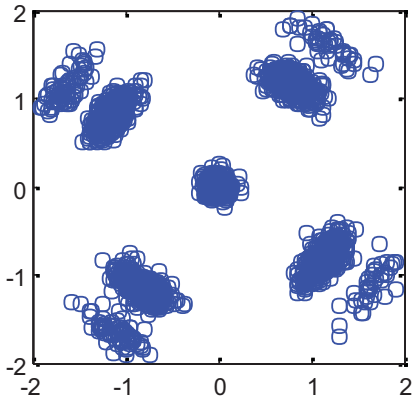

(e) x-polarization after coherent receiver

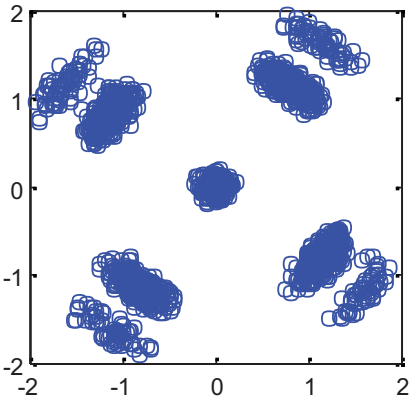

(f) y-polarization after coherent receiver

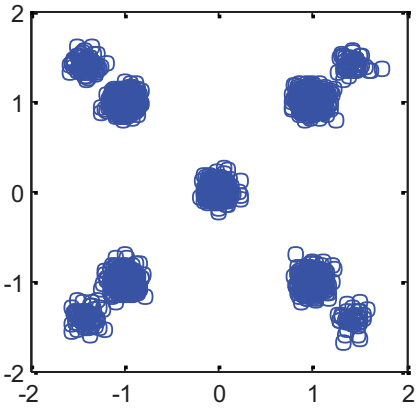

(g) x-polarization compensated by V&V

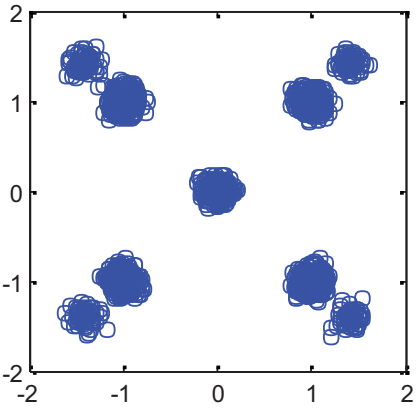

(h) y-polarization compensated by V&V

Figure 4.3(a)-(h) POL-QAM 6-4 constellation changes in a fiber system considering laser phase noise effect and compensation algorithms

Figure 4.4 (a)-(h) shows an example of constellation change for 128-SP-QAM for a fiber

length L=400km. (g) and (h) prove that DD can also recover the phase noise from the received 128-SP-QAM signal. Figure 4.4 (a)(b) show the original constellations of 128-SP-QAM before transmission. (c)(d) show the phase offset effect where one can see that, laser phase noise affects 128-SP-QAM more than POL-QAM 6-4. (e)(f) show the effect of receiver noise, and (g)(h) show the phase offset is compensated by the DD algorithm. Note that in Figure 4.4 (a)-(h), 128-SP-QAM constellation is distorted in a fiber system considering laser phase noise effect and compensated by the DD phase recovery algorithm.

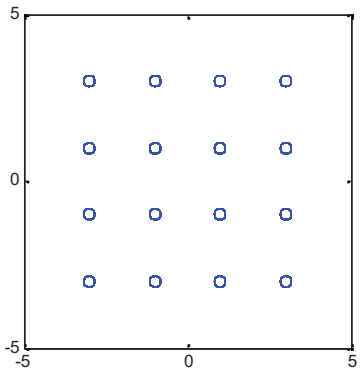

(a) 128-SP-QAM x-polarization

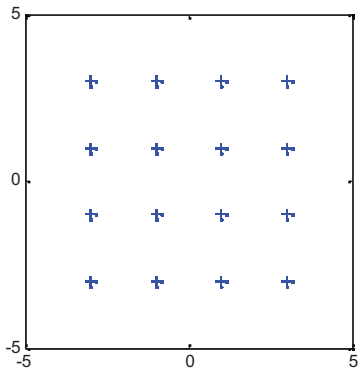

(b) 128-SP-QAM y-polarization

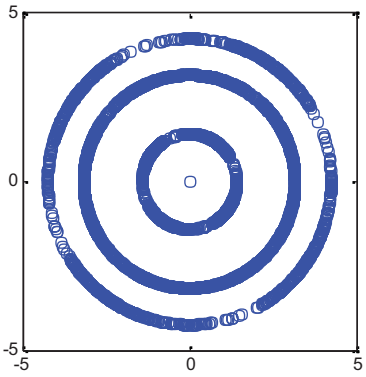

(c) x-polarization under laser phase noise

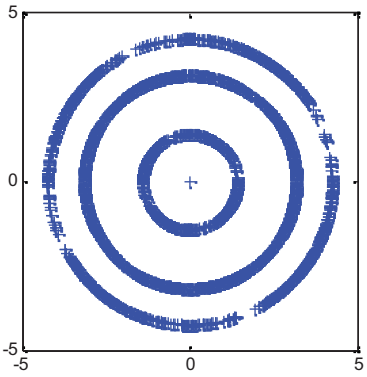

(d) y-polarization under laser phase noise

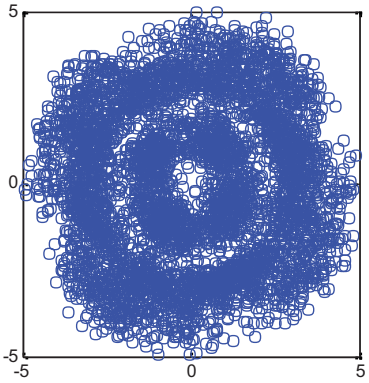

(e) x-polarization after coherent receiver

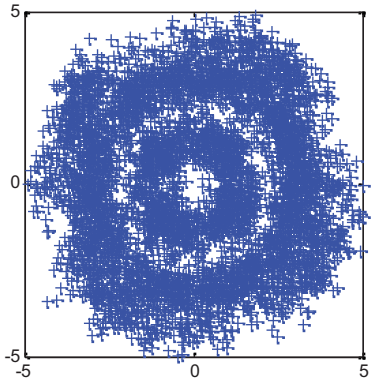

(f) y-polarization after coherent receiver

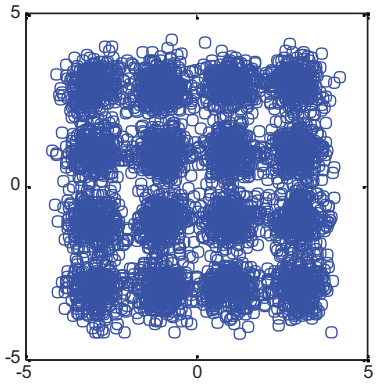

(g) x-polarization compensated by DD

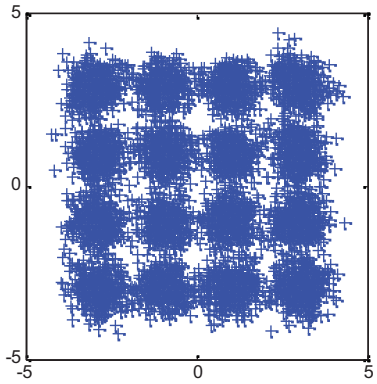

(h) y-polarization compensated by DD

Figure 4.4 (a)-(h) 128-SP-QAM constellation changes in a fiber system

The BER performance of POL-QAM 6-4 is shown in Figure 4.5 when compensated by DD and V&V algorithms. It is shown that DD performs slightly better than V&V in longer transmission distances (i.e., low SNR). This is because V&V uses a block of symbols to estimate a common phase error in every block and hence when the SNR is low, the phase error per block is large. One the other hand, the DD algorithm estimates the phase on symbol-by-symbol basis and hence better performance than the V&V at low SNR. However, at high SNR, both the V&V and the DD offer accurate phase estimates and hence better performance.

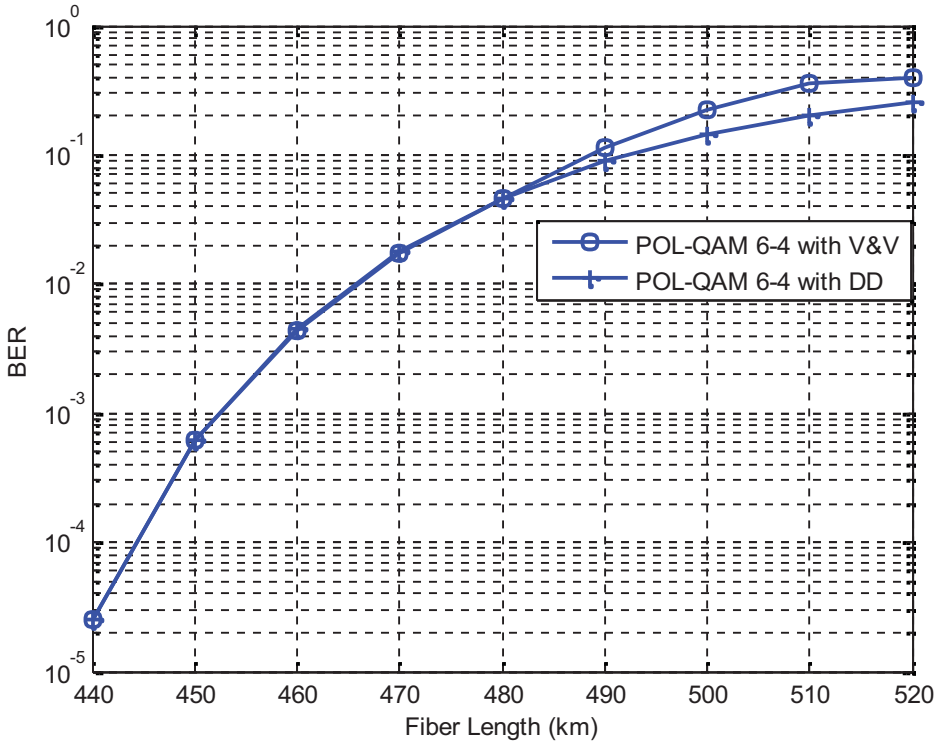

Figure 4.5 BER performances of POL-QAM 6-4 considering laser phase noise using carrier phase estimation algorithms with different fiber lengths

In Figure 4.6, we compare the BER performance of 128-SP-QAM with PDM-16QAM (Polarization Division Multiplexed 16-QAM), with DD carrier phase recovery. From the comparison, we can see that 128-SP-QAM outperforms PDM-16QAM since 128-SP-QAM employs non-differential coding.

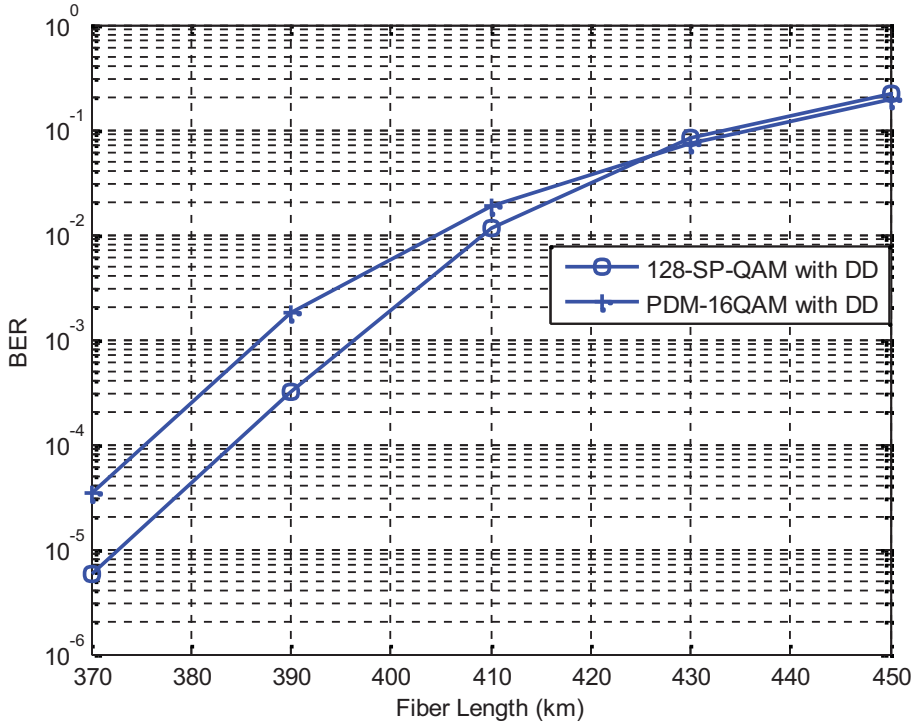

Figure 4.6 BER performances of 128-SP-QAM and PDM-16QAM considering laser phase noise using DD algorithm with different fiber lengths

4.4.2 Constellation Change in Long-Haul System

In this section, we simulate POL-QAM 6-4 and 128-SP-QAM in long-haul fiber communication systems. The total fiber length L=4500km with 45 EDFAs. POL-CMA and LMS step sizes are optimized which will be discussed later. Figure 4.7 (a)-(g) shows constellation change for POL-QAM 6-4. (a) shows the POL-QAM constellation at transmitter. (b) shows the phase offset effect. (c) shows the constellation change after 2000km transmission. (d) shows the signal at the receiver. (e)(f) show the POL-CMA and V&V algorithms to compensate for the phase distortion. As we can see from (g)-(h), the LMS is used to equalize the received signal.

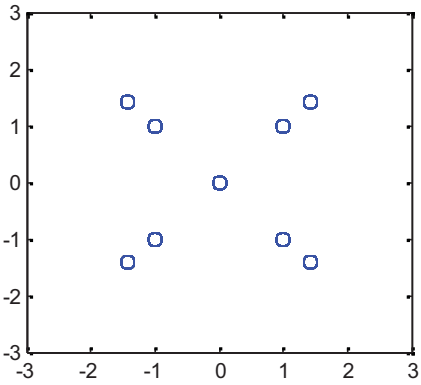

(a) POL-QAM 6-4 at transmitter

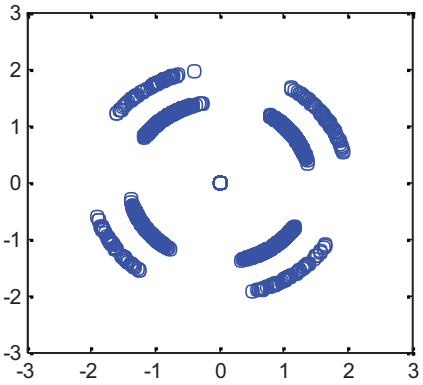

(b) After laser phase noise

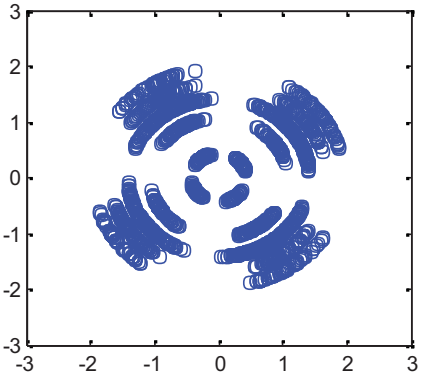

(c) Constellation at 2000km

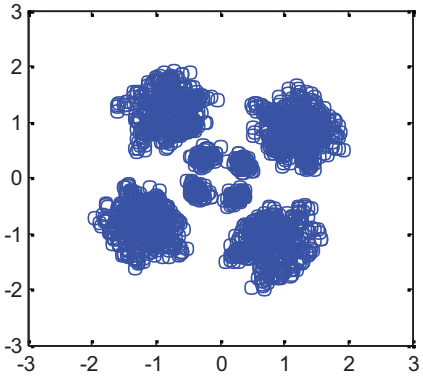

(d) Constellation at the receiver (4500km)

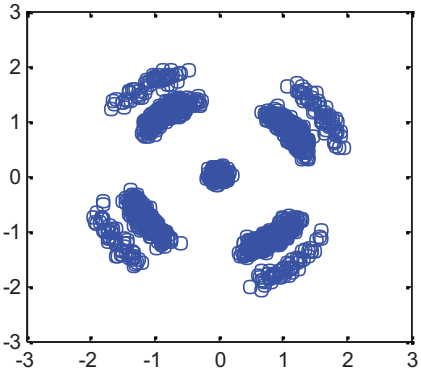

(e) Using POL-CMA equalization

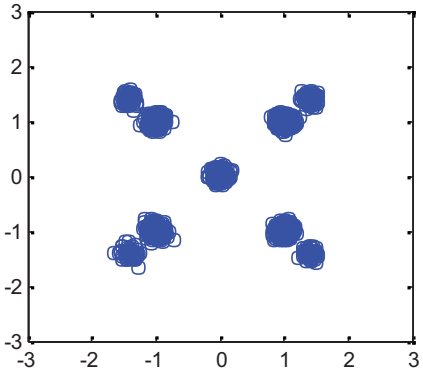

(f) After V&V phase compensation

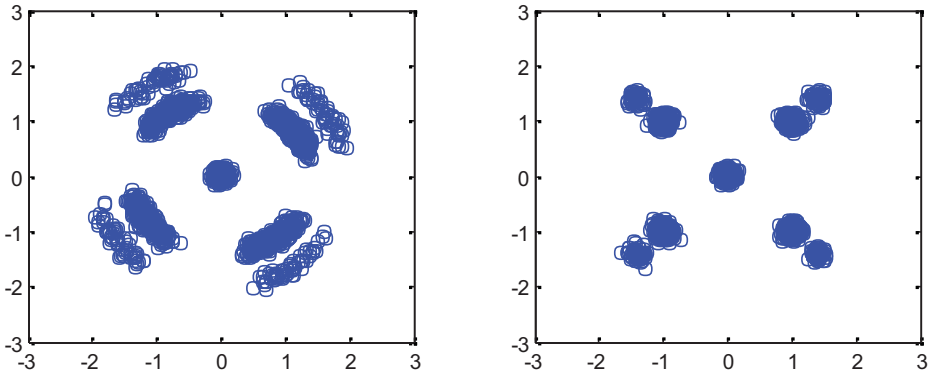

(g) Using LMS equalization (h) After V&V phase compensation

Figure 4.7 (a)-(h) POL-QAM 6-4 x-polarization constellation changes in long-haul system

We selected MMA and LMS as equalization methods (presented in chapter 3) for 128-SP-QAM and DD carrier phase recovery algorithm is used to estimate the carrier phase offset. The fiber length L=4700km. Fiber span length is 100km (implement a EDFA every 100km). The corresponding constellation diagram at the different system levels are shown in Figure 4.8. Figure 4.8(a) shows the 128-SP-QAM constellation at transmitter. (b) shows the phase offset effect. (c) shows the constellation change after 2000km transmission. (d) shows the signal at the receiver. (e)(f) show the MMA and DD compensation method. (g)(h) show the LMS method and DD algorithm.

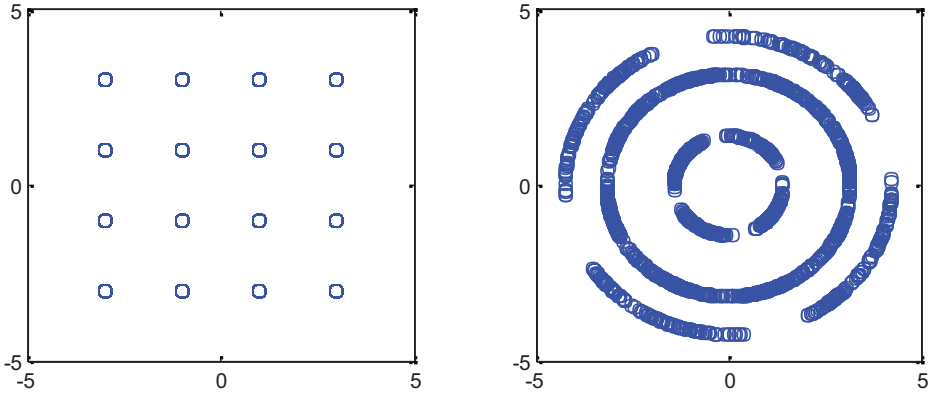

(a) 128-SP-QAM at transmitter

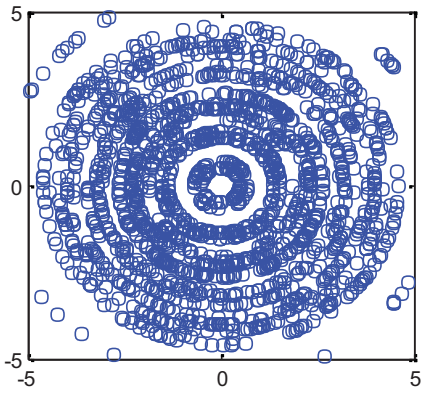

(b) After laser phase noise

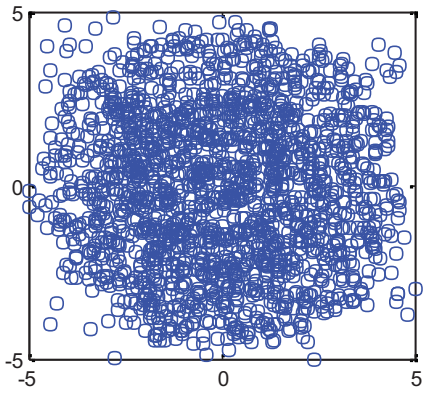

(c) Constellation at 2000km

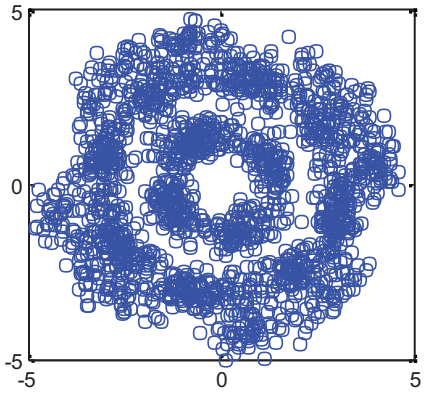

(d) Constellation at the receiver (4700km)

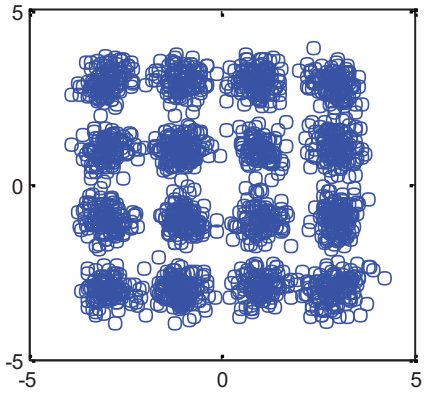

(e) Using MMA equalization

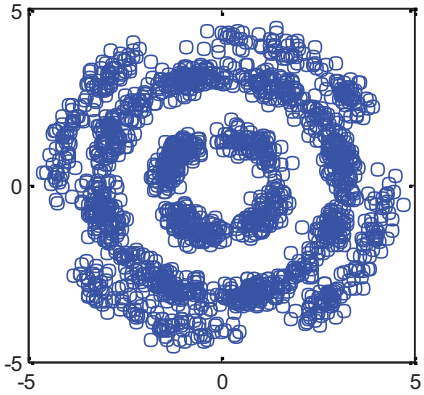

(f) After DD phase compensation

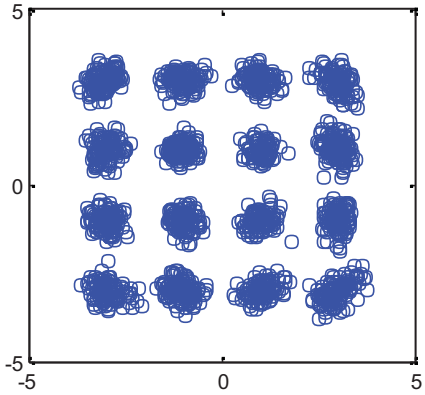

(g) Using LMS equalization

(h) After DD phase compensation

Figure 4.8 (a)-(h) 128-SP-QAM x-polarization constellation changes in long-haul system

4.4.3 Equalizer Step Size Optimization

In this section, we optimize the step size of the equalizer to improve the system performance. Figure 4.9 shows the BER performances with different step sizes for the POL-CMA and LMS considering POL-QAM 6-4 modulation. The transmission distance L=5200km (52 EDFAs). Laser phase noise is considered and compensated by the V&V algorithm. The results also show that LMS has better performance than POL-CMA.

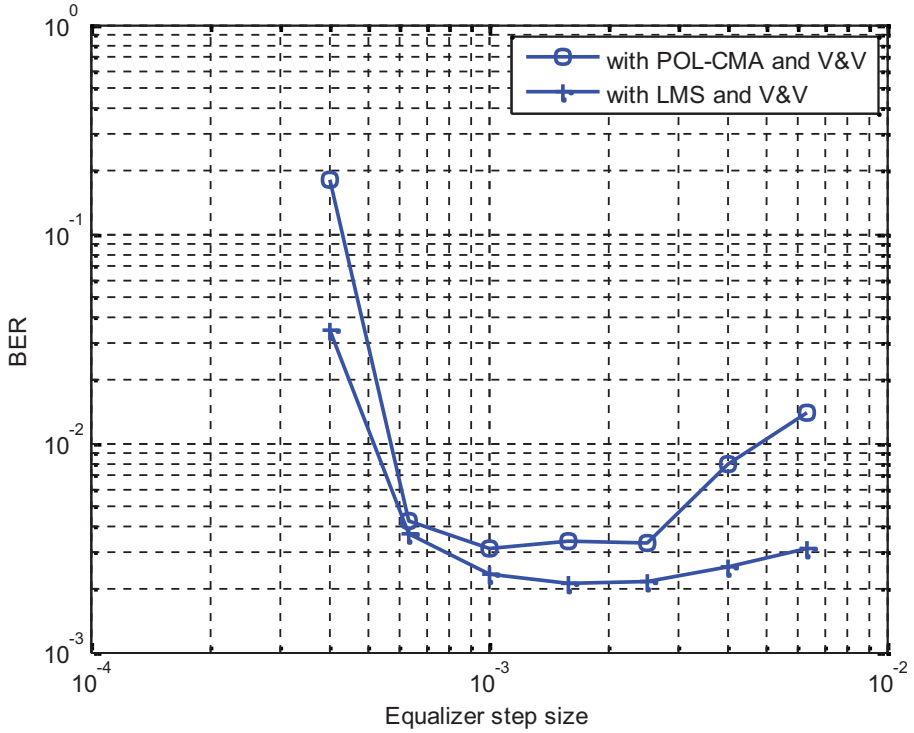

Figure 4.9 The BER performances with the step size of POL-CMA and LMS for POL-QAM

Figure 4.10 shows the performance of both MMA and LMS for 128-SP-QAM as a function of the step size. The transmission distance L=5200km (52 EDFAs).

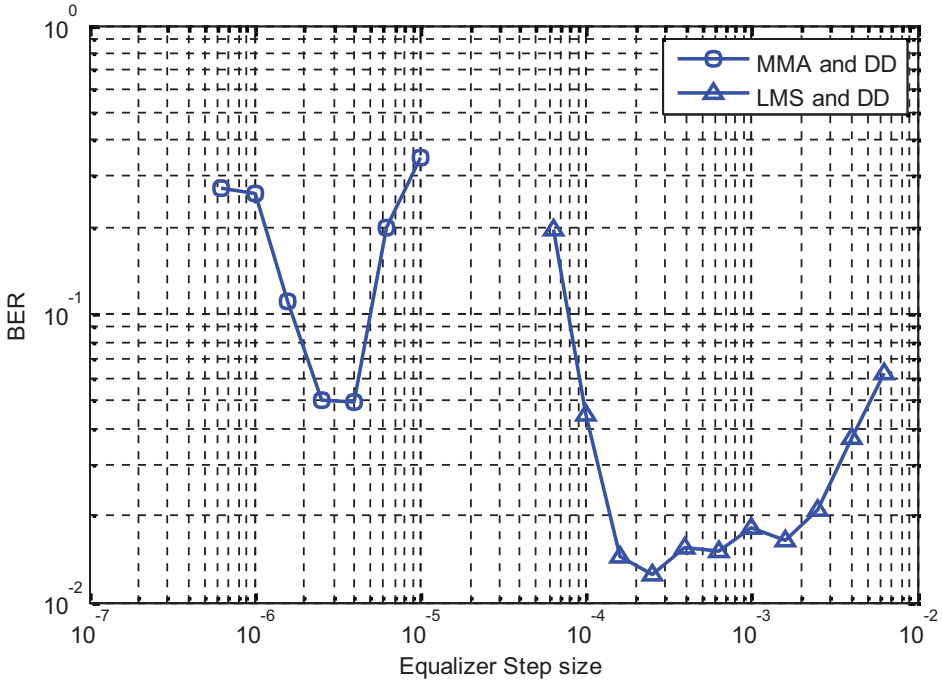

Figure 4.10 The BER performances with the step size of MMA and LMS for 128-SP-QAM

4.4.3 System Performance with Different Transmission Length

Here we consider the step sizes for the equalizers are optimized and discuss the system performance under different fiber lengths with amplifier distance set to 100km. As the fiber length increases, the fiber attenuation increases and the number of EDFAs is increased which results in overall higher amplifier noise. This leads to lower SNR at the receiver.

In this simulation, the Reed-Solomon RS(511,455) encoded model is considered. In RS(n,k) code, n is the code length $n=2^m-1$, k is the length of the information message [65]. The encoding and decoding methods of RS codes are based on Galois Field (2^m). The RS encoder separates the original data bits into groups and consider every m bits as a symbol (for POL-QAM 6-4, m=9, since there are 9 bits in 2 symbols.

Figure 4.11 presents the performance of POL-QAM 6-4 and PDM-4QAM modulations with different DSP algorithms. As seen, PDM-4QAM shows better performance than the uncoded POL-QAM 6-4. Also the RS(511,455) encoded POL-QAM 6-4 [23] offers the best performance relative to all other systems.

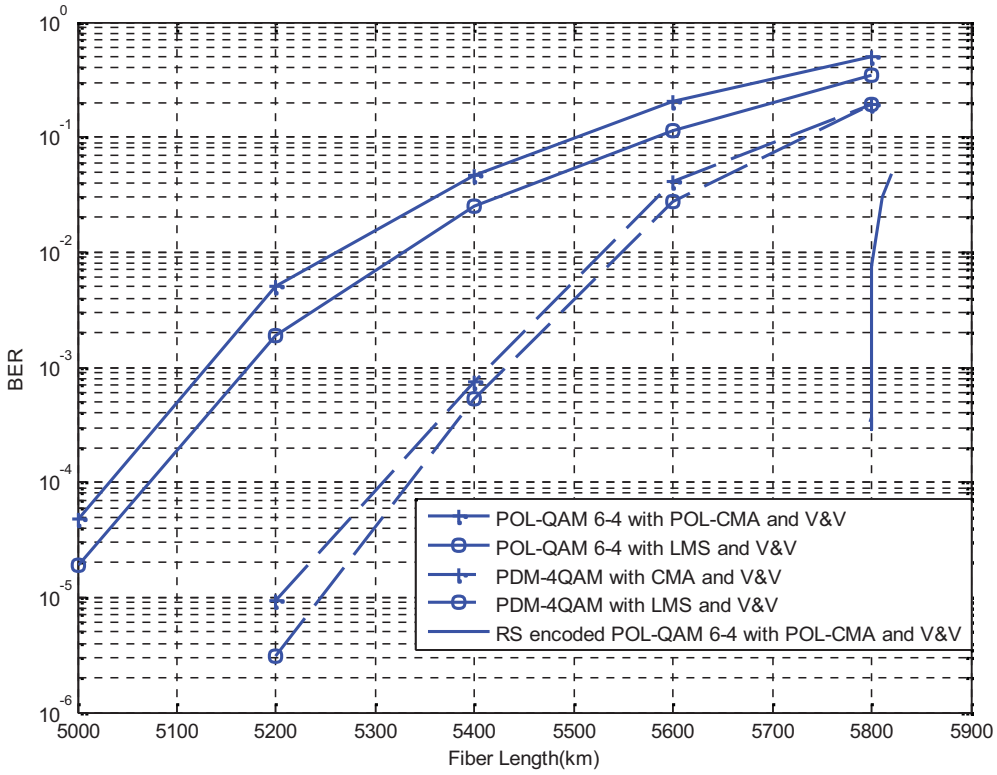

Figure 4.11 POL-QAM 6-4 and PDM-4QAM BER performance with different fiber length in long-haul systems

As we can see from Figure 4.12, 128-SP-QAM shows better performance than PDM-16QAM without losing spectral efficiency. This is seen as 128-SP-QAM offers a longer transmission range than PDM-16QAM at a specified BER when using LMS equalization and DD for phase compensation. Comparing the results of MMA and LMS for the 128-SP-QAM, LMS has a transmission range advantage compared with MMA.

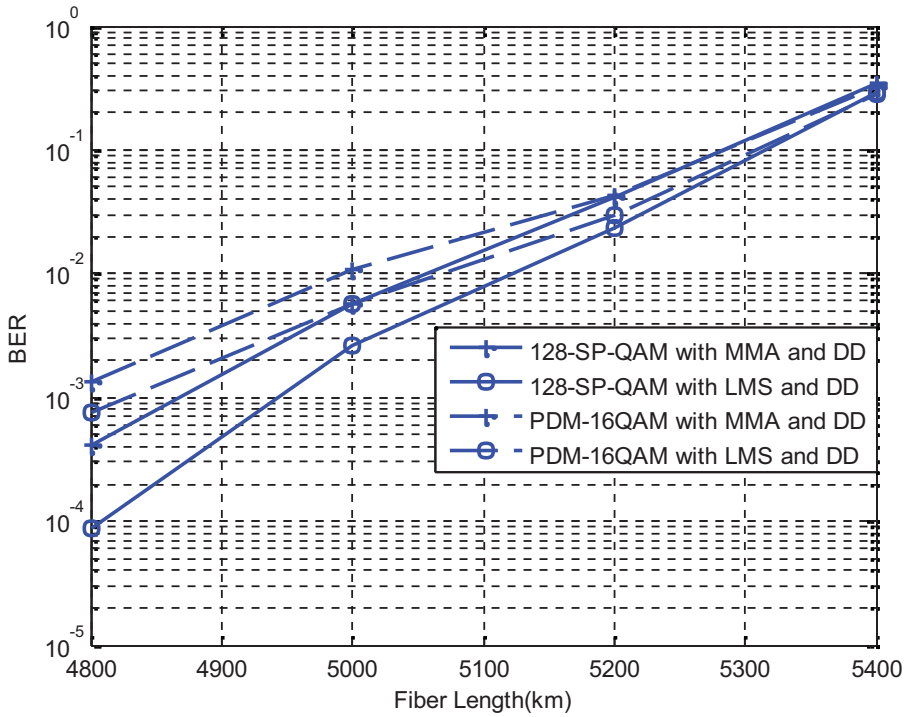

Figure 4.12 128-SP-QAM and PDM-16QAM BER performance with different fiber length in long-haul systems

4.4.4 System performance with different fiber lengths

In order to explore the effect of distance between each EDFA, we simulate the long-haul system with different fiber span length. We fixed the total fiber length L=5300km and change the number of EDFAs. The EDFA gain is tunable to fix the value of power loss (-0.75dB) in every fiber span. As we can see from Figure 4.13, as expected, the BER performance is better when there are more EDFAs in the long-haul system.

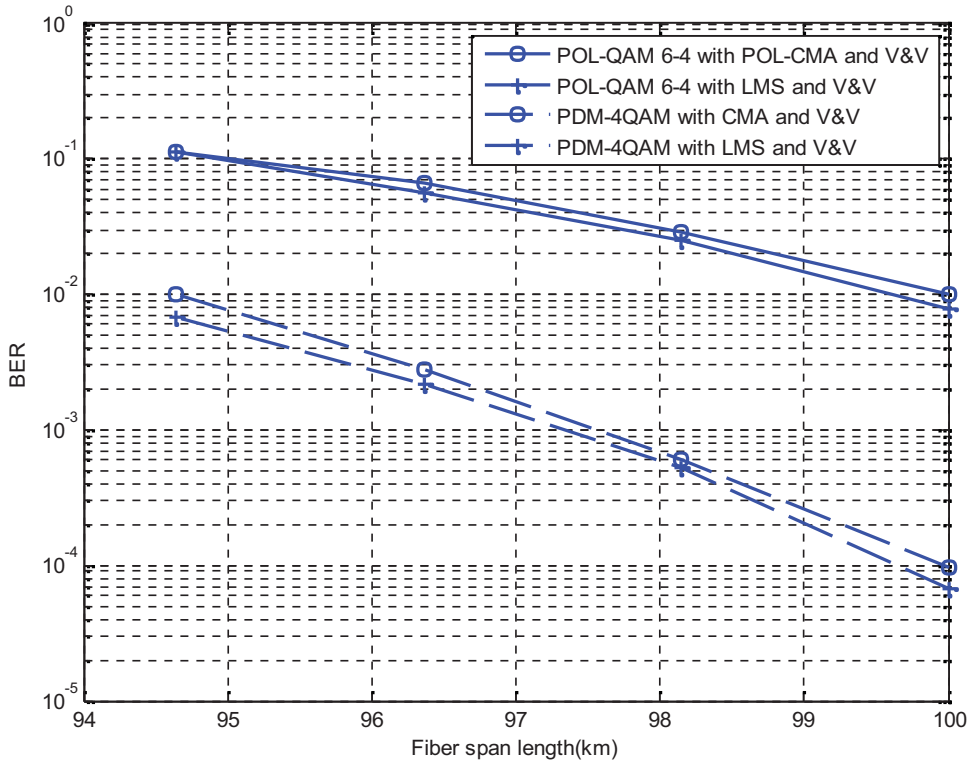

Figure 4.13 POL-QAM 6-4 and PDM-4QAM BER performance with different fiber span length in long-haul systems

For 128-SP-QAM, the simulation results are shown in Figure 4.14. The total fiber length L=5000km As we can see, PDM-16QAM performs slightly better than 128-SP-QAM when the fiber span length decreases.

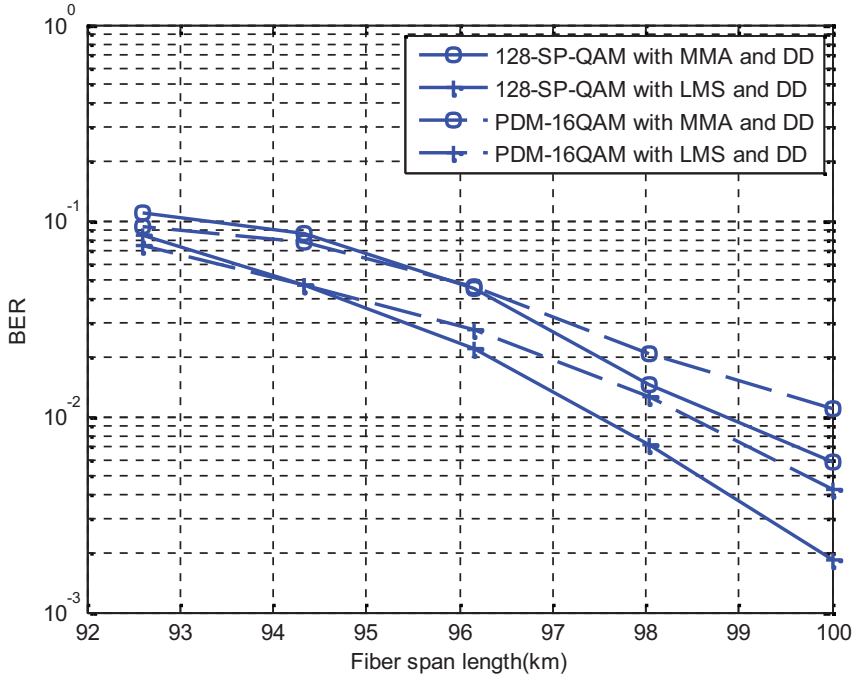

Figure 4.14 128-SP-QAM and PDM-16QAM BER performance with different fiber span length in long-haul systems

4.4.5 Amplifier Nonlinear Phase Noise

Amplifier phase noise can be described as linear phase noise and nonlinear phase noise. In this section, we investigate only the amplifier nonlinear phase noise

In addition to amplifier ASE noise, Gordon *et al*. [66] has shown that the optical amplifier noise and fiber Kerr effect distort the carrier phase. This effect is called amplifier nonlinear phase noise. The nonlinear phase noise caused by amplifiers is correlated with the received signal intensity and number of amplifiers described by [67]

$$\sigma_{\phi_{NL}}^2 = \frac{4}{3} N_{amp}(N_{amp} + 1)\sigma^2\left[(N_{amp} + \frac{1}{2})A^2 + (N_{amp}^2 + N_{amp} + 1)\sigma^2\right] \quad (4.4.5)$$

where N_{amp} is the number of amplifiers, σ^2 is the ASE noise variance per dimension per span (introduced in (4.2.1b)), A is the amplitude of the transmitted signal.

In this section, we consider EDFA with nonlinear phase noise. The system setup is introduced in section 4.3. The amplifier distance (fiber span length) is 100km. The BER performance of POL-QAM 6-4 and 128-SP-QAM in long-haul systems are shown in Figures 4.15, 4.16 respectively. We can see that under non-linear EDFA phase noise, the result of the simulation seems similar with Figure 4.11. The performance of PDM-4QAM is better than un-encoded POL-QAM 6-4.

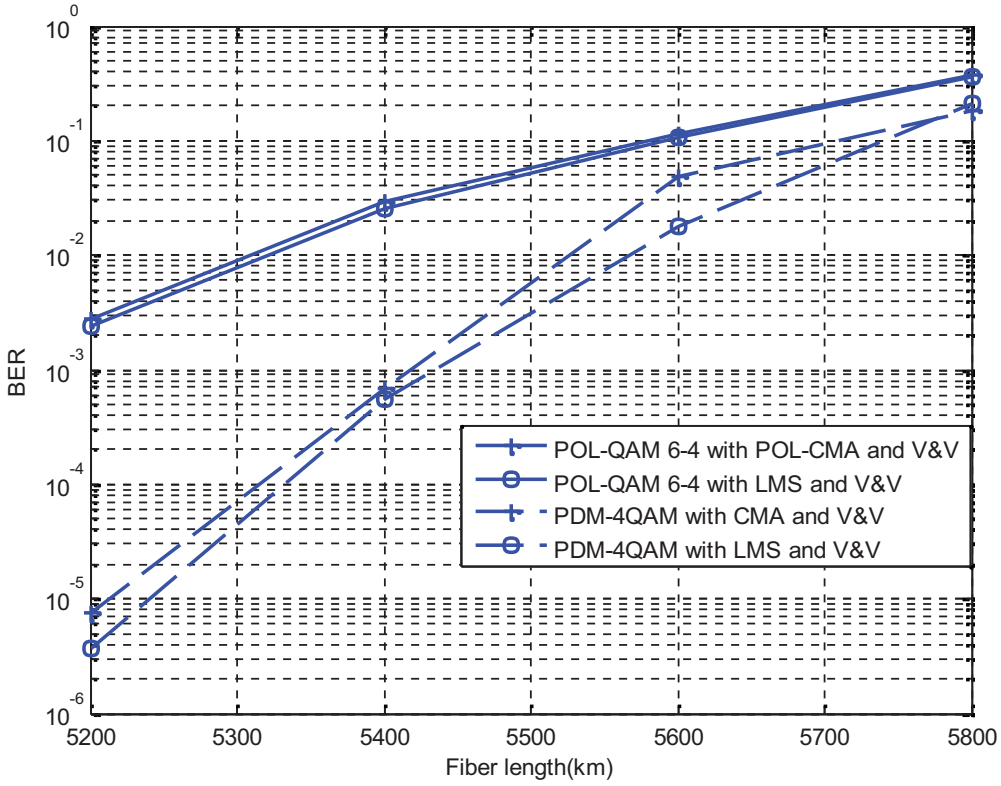

Figure 4.15 POL-QAM 6-4 and PDM-4QAM BER performance with different fiber length in long-haul systems, considering nonlinear phase noise as amplifier noise

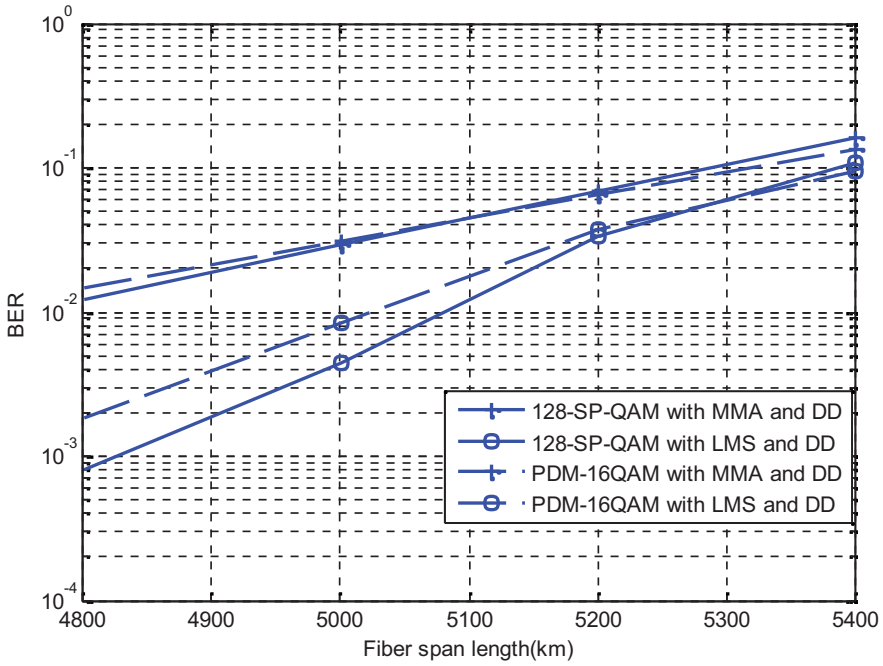

Figure 4.16 128-SP-QAM and PDM-16QAM BER performance with different fiber length in long-haul systems; considering nonlinear phase noise as amplifier noise

4.5 Conclusions

We investigated the performance of POL-QAM 6-4 and 128-SP-QAM in long-haul systems. We assumed laser phase noise, PMD effect, polarization rotation effect, EDFA amplification and also its ASE noise, which compensated by POL-CMA, LMS or MMA equalization algorithms and V&V or DD carrier phase estimation algorithms. Furthermore we analyzed BER performances of the two modulation formats under long-haul system simulations. It is shown that our POL-CMA works well with POL-QAM 6-4 in a long-haul system. However, MMA shows a non-negligible drawback in terms of its transmission range.

The un-coded POL-QAM 6-4 is shown to offer worse BER performance compared to PDM-4QAM due to its higher symbol alphabet. In contrast, the coded POL-QAM 6-4 has

a significant improvement in performance. On the other side, 128-SP-QAM performs better than PDM-16QAM except when the fiber span length is short.

Chapter 5

Conclusions and Future Works

6.1 Conclusions

In chapter 3, a modified CMA for the new modulation format POL-QAM 6-4 is proposed. Specifically, we simulated the BER performance of this new algorithm in a simplified channel. We also compared the result to LMS and found that the blind equalization algorithm POL-CMA without training sequence has less transmission range than LMS. Furthermore, another new modulation format 128-SP-QAM was analyzed in the same channel with MMA equalization. It shows great advantage of BER performance compared to PDM-16-QAM by employing non-differential coding.

In chapter 4, the long-haul optical transmission systems for POL-QAM and SP-QAM have been simulated and analyzed. We considered laser phase noise as an additive wiener process phase noise. The distortion of EDFA has been introduced as ASE noise and modeled as Gaussian distributed. To compensate for laser phase noise, carrier phase recovery DSP algorithms have been investigated. Furthermore, we have shown that our modified POL-CMA works well in long-haul systems, Also, the RS(511,455) encoded POL-QAM 6-4 shows significant improvement in transmission performance with

POL-CMA.

6.2 Future Directions

Although this thesis has investigated the BER performance of POL-QAM and SP-QAM over long-haul system, and proposed a modified CMA for POL-QAM (POL-CMA), there are still some works that remain to be studied. In this section, we list some important areas which need further studies.

- In chapter 3 and 4, nonlinear effects in the fiber (such as SPM, XPM *et al*.) are not considered due to the high complexity of the compensating implementations. However, the compensation of nonlinear effects for POL-QAM and SP-QAM is an interesting issue for future research.
- There are two methods to implement 128-SP-QAM which are non-differential coding and differential coding. It is of interest to consider differential coding as it is an important issue for 128-SP-QAM in the long-haul systems.

Bibliography

[1] R. Ramaswami, "Optical fiber communication: From transmission to networking," *Communications Magazine, IEEE*, vol. 40, pp. 138-147, May. 2002.

[2] T. H. Maiman, “Stimulated optical radiation in ruby,” *Nature Journal*, vol.187, pp. 493-494, Aug. 1960.

[3] K. C. Kao, G. A. Hockham, "Dielectric-fibre surface waveguides for optical frequencies," *Proc. Inst. Electr. Eng. Journal*, vol. 113, pp. 1151-1158, July. 1966.

[4] L. G. Kazovsky, S. Benedetto and A. E. Willner, *Optical fiber communication Systems*. London: Artech House, Jun. 1996.

[5] V. S. Bagad, I. A. Dhotre, *Data Communication and Networking*. India: Technical Publications, Jan. 2005.

[6] J. Gowar, *Optical communication systems*, Upper Saddle River, NJ: 2nd ed. Prentice Hall, 1993.

[7] M. Nakazawa, K. Kikuchi, T. Miyazaki, *High spectral density optical communication technologies*. vol. 6. Verlag Berlin Heidelberg-Springer, 2010.

[8] J. M. Kahn and K.-P. Ho, “Spectral efficiency limits and modulation/detection techniques for DWDM Systems,” *J. Sel. Top. Quantum Electron*, vol. 10, pp. 259-271, March/April. 2004.

[9] M. Schwartz, *Information transmission, modulation and noise. a unified approach to communication systems*. New York: McGraw-Hill, 1970.

[10] L. W. Couch, M. Kulkarni, and U. S. Acharya, *Digital and analog communication systems*. Upper Saddle River, NJ: Prentice Hall, 1997.

[11] B. P. Lathi, *Modern Digital and Analog Communication Systems*. New York: Oxford University Press, 1995.

[12] E. E. Basch, T. G. Brown, “Introduction to the coherent optical fiber transmission,” *IEEE Communications Magazine*, vol. 23, pp. 23-30, 1986.

[13] T. Okoshi, “Recent advances in coherent optical fiber communication systems,” *J. Lightwave Technol*., vol. LT-5, pp. 44-52, Jan. 1987.

[14] T. Kimura, "Coherent optical fiber transmission," *J. Lightwave Technol*., vol. LT-5, pp. 414-428, April. 1987

[15] T. Okoshi, *Coherent Optical Fiber Communications*. Tokyo: KTK Scientific Publishers (KTK), 1988.

[16] P. S. Henry, S. D. Personick, *Coherent Lightwave Communications.* Piscataway, NJ: IEEE Press, 1990.

[17] M. Awad, I. Dayoub, W. Hamouda, and J. M. Rouvaen, "Adaptation of the Mode Group Diversity-Multiplexing Technique for Radio Signal Transmission over MMF," *IEEE/OSA Journal of Optical Communications and Networking*, vol. 3, pp. 1-9, Jan. 2011.

[18] A. M. Foubat, I. Dayoub, J. M. Rouvaen, W. Hamouda, and M. Awad, "A Novel Approach for the Interference Cancellation in DS-CDMA Optical Networks," *IEEE/OSA Journal of Optical Communications and Networking*, vol. 1, pp. 204-212, Aug. 2009.

[19] M. Awad, W. Hamouda, and I. Dayoub, "Throughput Maximization Approach for O-MIMO Systems using MGDM Technique," *IEEE Global Telecommunications Conference (GLOBECOM 2012)*, LA, California, Dec. 2012.

[20] G. P. Agrawal, *Fiber-optic communication systems*. Hoboken, NJ: vol. 222, John Wiley & Sons, 2010.

[21] M. Schwartz, W. R. Bennett, and S. Stein, *Communication Systems and Techniques*. New York: McGraw-Hill, 1966.

[22] M. S. Roden, *Analog and Digital Communication Systems*. Upper Saddle River, NJ: Prentice Hall, 1995.

[23] H. Bülow, “Polarization QAM Modulation (POL-QAM) for Coherent Detection Schemes,” *2009 Conference on Optical Fiber Communication*, San Diego, CA, USA, March 2009.

[24] G. Ungerboeck, "Channel coding with multilevel/phase signals," *IEEE Trans. Inf. Theory*, vol. IT-28, pp. 55-67, Jan. 1982.

[25] G. Keiser, *Optical Fiber Communication.* New York: McGraw-Hill, 1983.

[26] B. W. Hakki, "Polarization mode dispersion in a single mode fiber," *J Lightwave Technol*, vol. 14, pp.2202-2208, Oct. 1996.

[27] C. D. Poole and R. E. Wagner, "Phenomenological approach to polarization dispersion in long single-mode fibers," *Electron. Lett.*, vol. 22, pp. 1029-1030, Sep. 1986.

[28] D. Andresciani, F. Curti, F. Matera, and B. Diano, "Measurement of the group-delay difference between the principal states of polarization on a low-birefringence terrestrial fiber cable," *Optics Lett.*, vol. 12, pp. 844-846, Oct. 1987.

[29] G. J. Foschini, C. D. Poole, "Statistical theory of polarization dispersion in single mode fibers," *J. Lightwave Technol.*, vol. 9, pp.1439-1456, Nov. 1991.

[30] C. D. Poole, J. H. Winters, and J. A. Nagel, "Dynamical equation for polarization dispersion," *Optics Lett.*, vol. 16, pp. 372-374, Mar. 1991.

[31] B. L. Heffner, "Automated measurement of polarization mode dispersion using Jones matrix eigenanalysis," *IEEE Photonics Technol. Lett.*, vol. 4, pp. 1066-1069, Sept. 1992.

[32] S. C. Rashleigh, "Origins and control of the polarization effects in single-mode fibers," *J. Lightwave Technol.*, vol. LT-1, pp. 312-331, June 1983.

[33] S. J. Savory, "Digital filters for coherent optical receivers," *Opt. Express Journal*, vol. 16, pp. 804-817, Jan. 2008.

[34] E. Ip, A. P. T. Lau, D. J. F. Barros, J. M. Kahn, "Coherent detection in optical fiber systems," *Optics Express (USA) Journal*, vol. 16, pp. 753-791, Jan. 2008.

[35] D. S. Millar, D. Lavery, S. Makovejs, C. Behrens, B. C. Thomsen, P. Bayvel, and S. J. Savory, "Generation and long-haul transmission of polarization-switched QPSK at 42.9 Gb/s," *Optics Express (USA) Journal*, vol. 19, No. 10, pp. 9296-9302, May. 2011.

[36] H. G. Batshon, I. Djordjevic, T. Schmidt, "Ultra high speed optical transmission using subcarrier-multiplexed four-dimensional LDPC-coded modulation," *Optics Express*, vol. 18, pp. 20546-20551, Sept. 2010.

[37] L. D. Coelho, N. Hanik, “Global optimization of fiber-optic communication systems using four-dimensional modulation formats,” *European Conference on Optical Communication, ECOC*, Geneva, Switzerland, 2011.

[38] M. Sjodin, P. Johannisson, J. Li, P. A. Andrekson, E. Agrell, and M. Karlsson, “Comparison of 128-SP-QAM with PM-16-QAM,” *Optics Express (USA) Journal*, vol. 20, pp. 8356–8366, April 2012.

[39] M. Karlsson, E. Agrell, “Which is the most power-efficient modulation format in optical links?” *Optics Express (USA) Journal*, vol. 17, pp. 10814–10819, 2009.

[40] M. Karlsson, E. Agrell, “Spectrally efficient four-dimensional modulation,” *2012 OFC Collocated National Fiber Optic Engineers Conference*, Los Angeles, CA, USA, 2012.

[41] J. H. Conway, N. J. A. Sloane, “Fast quantizing and decoding algorithms for lattice quantizers and codes,” *IEEE Trans. Inf. Theory*, vol. 28, pp. 227–232, Mar. 1982.

[42] J. Salz, “Modulation and detection for coherent lightwave communications,” *IEEE Communications Magazine*, vol. 24, pp. 38-49, Jun. 1986.

[43] A. J. Viterbi, A. M. Viterbi, “Nonlinear Estimation of PSK-Modulated Carrier Phase with Application to Burst Digital Transmission,” *IEEE Trans Inf. Theory*, vol. IT-29, pp. 543-551, July 1983.

[44] S. P. Singh, N. Singh, “Nonlinear effects in optical fibers: Origin, Management and applications,” *progress in electromagnetic research*, vol. 73, pp. 249-275, 2007

[45] G. P. Agrawal, *Nonlinear Fiber Optics*. New York: 4th ed, Academic Press, 2007.

[46] S. Mumtaz, René-Jean Essiambre, and G. P. Agrawal, "Nonlinear propagation in multimode and multicore fibers: generalization of the Manakov equations," *Journal of Lightwave Technology*, vol. 3, pp. 398-406, 2013.

[47] D. Rafique, M. Mussolin, M. Forzati, J. Martensson, M. N. Chugtai, A. D. Ellis, "Compensation of intra-channel nonlinear fibre impairments using simplified digital back-propagation algorithm," *Optics express*, vol. 19, pp. 9453-9460, May. 2011.

[48] G. Goldfarb, M. G. Taylor and G. Li, “Experimental demonstration of fiber impairment compensation using the split-step finite-impulse-response filtering method,” *IEEE Photon. Technol. Lett.*, vol. 20, pp. 1887-1889, Nov. 2008.

[49] F. Yaman, G. Li, “Nonlinear impairment compensation for polarization-division multiplexed WDM transmission using digital backward propagation,” *IEEE Photonics J.*, vol. 2, pp. 816-832, Oct. 2010.

[50] D. J. Malyon, T. G. Hodgkinson, D. W. Smith, R. C. Booth, and B. E. Daymond-John, “PSK homodyne receiver sensitivity measurements at 1.5 ÎOEm,” *Electronics Letters*, vol. 19, pp. 144-146, Feb. 1983.

[51] R. A. Linke, B. L. Kasper, N. A. Olssson, and R. C. Alferness, “Coherent lightwave transmission over 150 km fibre lengths at 400 Mbit/s and 1 Gbit/s data rates using phase modulation,” *Electronics Letters*, vol. 22, pp. 30–31, Jan. 1986.

[52] G. Nicholson, “Probability of error for optical heterodyne DPSK system with quantum phase noise,” *Electronics Letters*, vol. 20, pp. 1005 –1007, Nov. 1984.

[53] Y. Li, W. Rao, "Novel Blind Equalizer Based on SE-CMA and DD Algorithm," 2012 International Conference on Environmental Engineering and Technology, Ba ngkok, Thailand, 2012.

[54] Ram Babu, T., and P. Rajesh Kumar, "Blind Equalization using Constant Modulus Algorithm and Multi-Modulus Algorithm in Wireless Communication Systems," *International Journal of Computer Applications*, number 3, article 6, pp. 40-45, Feb. 2010.

[55] I. Fatadin, S. J. Savory, “Blind Equalization and Carrier Phase Recovery in a 16-QAM Optical Coherent System,” *Journal of lightwave technology*, vol. 27, pp. 3042-3049, Aug. 2009.

[56] D. N. Godard, “Self-recovering equalization and carrier tracking in two-dimensional data communication systems,” *IEEE Trans. Commun.*, vol. 28, pp. 1867–1875, Nov. 1980.

[57] J.Yang, J. J. Werner, G. A. Dumont, “The multimodulus blind equalization algorithm,” *13th International Conference on DSP*, vol.1, pp.127-130, July 1997.

[58] S. Wen, L. Feng, "A computationally efficient multi-modulus blind equalization algorithm," *2nd IEEE International Conference on Information Management and Engineering*, vol. 3, pp. 685-687, 2010.

[59] B. L. Heffner, “Automated measurement of polarization mode dispersion using Jones

matrix eigenanalysis," *IEEE Photon. Tech. Lett.*, vol. 4, pp. 1066-1069, Sept. 1992.

[60] K. Kikuchi, S. Tsukamoto, "Evaluation of sensitivity of the digital coherent receiver," *Journal of Lightwave Technology*, vol. 26, pp. 1817-1822, July 2008.

[61] S. J. Savory, "Digital Coherent Optical Receivers: Algorithms and Subsystems," *IEEE J. Sel. Top. Quantum Electron.*, vol. 16, pp. 1164–1179, Sept.-Oct. 2010.

[62] J. G. Proakis, S. Masoud, *Communication systems engineering*. Upper Saddle River, New Jersey: 2nd ed. Prentice-Hall, 2002.

[63] E. Desurvire, J. R. Simpson, P. C. Becker, "High-gain erbium-doped traveling-wave fiber amplifier," *Optics Letters*, vol. 12, pp. 888-890, Nov. 1987.

[64] A. P. T. Lau, J. M. Kahn, "Design of inline amplifier gains and spacings to minimize the phase noise in optical transmission systems," *Journal of lightwave technology*, vol. 24, pp. 1334-1341, Mar. 2006.

[65] Xi, Su, Guo Ying, "The Application of RS code in CCK Modulation Technology," *1st International Conference on Information Science and Engineering*, Nanjing, China, Dec. 2009.

[66] J. P. Gordon, L. F. Mollenauer, "Phase noise in photonic communications systems using linear amplifiers," *Optics letters*, vol. 15, pp. 1351-1353, Dec.1990.

[67] Ho, Keang-Po, "Probability density of nonlinear phase noise," *Journal of the Optical Society of America B: Optical Physics*, vol. 20, pp. 1875-1879, Sep. 2003.